

Hot Micro-Embossing of Thermoplastic Elastomers

By

Megan Firko

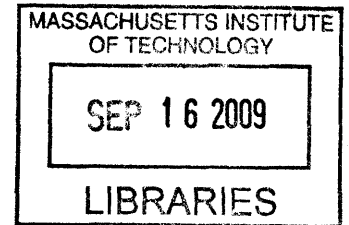
Submitted to the Department of Mechanical Engineering
in Partial Fulfillment of the Requirements for the Degree of

Bachelor of Science in Mechanical Engineering

at the

Massachusetts Institute of Technology

June 2008



ARCHIVES

© Massachusetts Institute of Technology
All Rights Reserved

Signature of Author

A handwritten signature in black ink, appearing to be "Megan Firko".

Department of Mechanical Engineering
May 9, 2008

Certified by

A handwritten signature in black ink, appearing to be "David E. Hardt".

David E. Hardt
Ralph E. and Eloise F. Cross Professor of Mechanical Engineering
Thesis Supervisor

Accepted by :

A large, bold handwritten signature in black ink, appearing to be "John H. Leinhard, V.". The signature is written over a dotted line.

Professor John H. Leinhard, V.
Chairman; Undergraduate Thesis Committee

Hot Micro-Embossing of Thermoplastic Elastomers
by

Megan Firko

Submitted to the Department of Mechanical Engineering on May 9, 2008
in Partial Fulfillment of the Requirements for the Degree of
Bachelor of Science in Mechanical Engineering

ABSTRACT

Microfluidic devices have been a rapidly increasing area of study since the mid 1990s. Such devices are useful for a wide variety of biological applications and offer the possibility for large scale integration of fluidic chips, similar to that of electrical circuits. With this in mind, the future market for microfluidic devices will certainly thrive, and a means of mass production will be necessary. However PDMS, the current material used to fabricate the flexible active elements central to many microfluidic chips, imposes a limit to the production rate due to the curing process used to fabricate devices. Thermoplastic elastomers (TPEs) provide a potential alternative to PDMS. Soft and rubbery at room temperature, TPEs become molten when heated and can be processed using traditional thermoplastic fabrication techniques such as injection molding or casting. One promising fabrication technique for TPEs is hot micro-embossing (HME) in which a material is heated above its glass transition temperature and imprinted with a micromachined tool, replicating the negative of the tools features. Thus far, little research has been conducted on the topic of hot embossing TPEs, and investigations seeking to determine ideal processing conditions are non-existent. This investigation concerns the selection of a promising TPE for fabrication of flexible active elements, and the characterization of the processing window for hot embossing this TPE using a tool designed to form long winding channels, with feature heights of 66 μ m and widths of 80 μ m. Ideal processing conditions for the tool were found to be pressures in the range of 1MPa-1.5MPa and temperatures above 140°. The best replication occurred at 150°C and 1.5 MPa, and at these conditions channel depth was within 5% of the tool, and width was within 10%. For some processing conditions a smearing effect due to bulk material flow was observed. No upper limit on temperature was found, suggesting that fabrication processes in which the material is fully melted may also be suitable for fabrication of devices from TPEs.

Thesis supervisor: David E. Hardt
Title: Professor of Mechanical Engineering

Table of contents

Table of contents.....	3
List of figures.....	5
1 Introduction.....	7
1.1 Overview of Microfluidic Devices.....	7
1.2 Active Elements in Microfluidic Devices.....	10
1.2.1 Overview of active elements.....	10
1.2.2 Material Selection.....	12
1.3 Thesis Overview.....	14
2 Background.....	15
2.1 Thermoplastic Elastomers.....	15
2.1.1 Overview of Thermoplastic Elastomers.....	15
2.1.2 Previous use of TPEs for Microfluidic Applications.....	16
2.1.3 TPE Selection for the Current Investigation.....	17
2.2 Hot Micro-embossing.....	21
2.2.1 Overview of HME.....	21
2.2.2 Past Examples of HME.....	23
3 Experimental Method.....	25
3.1 HME Machine.....	25
3.2 Mold.....	26
3.3 Procedure for Tests.....	29
3.4 Measurement and Data Processing.....	31
4 Results and Discussion.....	36
4.1 Introduction.....	36
4.2 Criteria Used to Analyze Parts.....	36
4.3 Processing Window.....	38
4.4 Channel Formation.....	43
4.4.1 Smearing and Bulk Material Flow.....	44
4.5 Visual Confirmation from SEMs.....	51
4.6 Measurement Repeatability.....	54
5 Conclusions and future work.....	56
5.1 Summary.....	56
5.2 Conclusion.....	57
5.3 Future work.....	57
Appendix.....	59
A Cross Section Matrices.....	60
A.1 Matrix for Location 1.....	60
A.2 Matrix for Location 2.....	61
A.3 Matrix for Location 3.....	62
A.4 Matrix for Location 4.....	63
B Success of Part Formation.....	64
B.1 Average Width and Depth of Parts.....	64
B.2 Average Width and Depth of Tool.....	64
B.3 Location Specific Information.....	65

B.4 Success in Each Criteria.....	68
References.....	69

List of figures

Figure 1-1 A microfluidic device featuring LSI. Adapted from [3].	9
Figure 1-2 A simple valve that uses pressurized expansion of a control channel to seal a fluid duct [6]	11
Figure 1-3 The valve from figure 1-2 arranged to function as a simple valve (a), in series to create a pump (b), and in series on a closed loop to create a mixer (c) [6]	12
Figure 2-1A TPE with a polystyrenic hard phase. The polystyrene domains act as crosslinks for the elastomer. [10].	16
Figure 2-2 A table comparing the properties of PDMS and a number of TPEs.	20
Figure 2-3 Processing steps for hot micro-embossing. The polymer workpiece is shown in gray, while the micromachined tool is black [26]	22
Figure 2-4 Temperature and force trajectory during HME. Force is shown by the solid line and temperature is shown by the dashed line. [26].	23
Figure 3-1 HME machine	25
Figure 3-2 Schematic of the tool used for hot embossing.	27
Figure 3-3 Photo of the tool, showing tool size.	28
Figure 3-4 SEM image of the tool, showing a detailed view of tool features.	29
Figure 3-5 Schematic of the stack setup used for embossing.	30
Figure 3-6 Schematic of the tool showing measurement locations.	31
Figure 3-7 A Gwyddion window showing the typical step fitting function applied to a cross section.	33
Figure 3-8 A Gwyddion window showing the step fitting function for an uneven profile.	34
Figure 3-9 A Gwyddion 3D topography rendering of a part embossed at 130°C and 1MPa.	35
Figure 4-1 A part, embossed at 150°C and 2MPa, that displays bulk warping.	38
Figure 4-2 Processing window for Stevens Urethane 1880.	39
Figure 4-3 Processing window for Stevens Urethane 1880.	40
Figure 4-4(a) Gwyddion image of a channel embossed at 100°C and 0.25MPa. The channel is shallow and wide, and the surface is visibly rough. (b) SEM image of a channel embossed at 140°C and 1MPa. The residual surface texture from the TPE film is visible.	42
Figure 4-5Superimposed cross-sections for parts embossed at 140°C and a variety of pressures.	43
Figure 4-6 Photo of a part, embossed at 120°C and 4MPa, that demonstrates smearing.	45
Figure 4-7 SEMs of the same location on two different parts. (a) A channel without smearing, embossed at 140°C and 1MPa. (b) A channel that shows smearing, embossed at 130°C and 1MPa	46
Figure 4-8 Superimposed cross-sections for parts embossed at 0.5 MPa (a), 2MPa (b), and a variety of temperatures.	48
Figure 4-9 Illustration of the effect of bulk material flow on channel formation. The tool is shown in light gray, the part being embossed is black. The dark gray arrows represent material flow.	49

Figure 4-10 SEM image indicating radial flow direction. The smeared edge is perpendicular to flow, while the well formed edge is parallel..... 51

Figure 4-11 SEM images of the same location on the tool (a), a part embossed at 140° C and 1MPa (b), and a part embossed at 130° C and 2MPa (c). 53

1 Introduction

1.1 Overview of Microfluidic Devices

The development of microfluidic devices, also known as micro total analysis systems (μ TAS) or “lab on a chip” systems, has been a rapidly growing field since the mid 1990s [1, 2]. In the decade since they came to prominence, microfluidic devices have proven useful in a wide variety of biological applications, including separation of biological samples [2, 3], analysis of DNA through polymerase chain reaction (PCR) [2-4], flow cytometry [2], enzymatic assays [3], and numerous other applications involving the handling of cells and biomolecules [2, 3]. Microfluidic chips are appealing for biological applications in large part because one device can incorporate numerous functions. Thus, a single analysis system can perform pretreatment of a sample, a variety of separation and analysis techniques, and detection, as well taking measurements and controlling mass transport. This integration of elements allows a single device to monitor a number of components simultaneously [2, 5].

In addition to integrated system analysis, microfluidic devices provide a number of other features that can be superior to their macro scale counterparts. Some of these advantages stem from the small volumes of fluid manipulated by microfluidic devices. These volumes are on the order of micro- and even nano-liters, reducing the consumption of samples, reagents, and other fluids processed by the system [1, 2, 5]. In some instances, the physics of such small volumes can also lead to faster reaction and mixing times, or improve sensitivity and accuracy [1, 5]. Further advantages of microfluidic

systems over standard systems result from their small size. Such devices are more portable than full size analysis systems, allowing for real time or *in situ* analysis. Also, the small material consumption for each chip fabricated makes one time use, disposable parts more feasible, which is particularly advantageous for many biological applications [1].

Further motivation to develop microfluidic devices arises from the comparison to electronic circuits [1, 3]. In the first half of the 1900s, electronic circuits were constructed from individual components, such as vacuum tubes and, later, transistors. Each component had to be hand-soldered, an expensive, sometimes unreliable process which limited the complexity of the circuits that could be physically constructed. Then, in the late 1950s, integrated circuits were developed. These circuits incorporated a number of components, such as transistors, resistors, and capacitors, fabricated from a single semiconductor, thus eliminating many of the problems associated with manual assembly. By the middle of 1970, improved technology made it possible to create such circuits with hundreds or even thousands of individual components, so called large scale integration (LSI) [3]. A similar process is currently taking place with microfluidic devices. Fluidic technology employed in laboratories during the first part of this decade can be likened that of electronics prior to the creation of integrated circuits. These early stages of biological automation consist of entire rooms filled with machines to process fluids, as well as robotic handling systems to move fluid samples between machines. However, as the decade progresses and microfluidic technology improves, the move towards large scale integration for microfluidic devices becomes increasingly imminent

[1, 3]. Already, some microfluidic devices featuring LSI have been fabricated, such as that demonstrated by Thorson et.al, an image of which can be seen in figure 1-1.

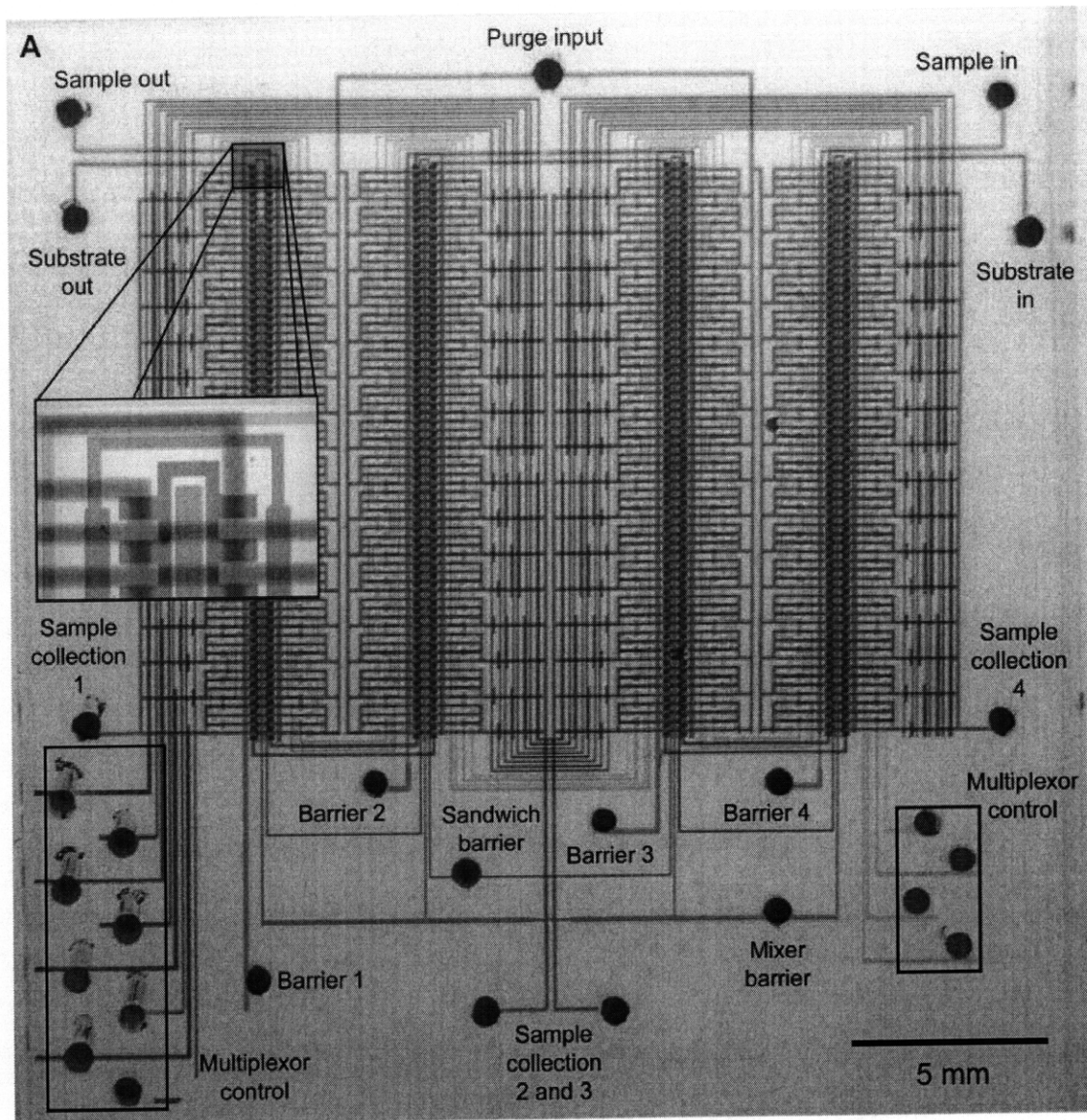


Figure 1-1 A microfluidic device featuring LSI. Adapted from [3].

This microfluidic device consists of 256 reaction chambers that act as fluidic comparators, and has been successfully used by its creator to test for the expression of enzymes. Crucial to the large scale integration and complex fluid manipulations achieved by this circuit are 2056 microvalves arranged to act as multiplexors [3]. Such

valves have been identified as a critical component for LSI and for the development of microfluidic systems that can rival the current robotic automation in practical applications [1, 3].

1.2 Active Elements in Microfluidic Devices

1.2.1 Overview of active elements

In microfluidic devices, active elements such as valves and pumps play a crucial role in fluid manipulation. These active elements can take on a wide variety of forms and methods of actuation, many of which are described by Reyes et. al. in their overview of μ TAS [2]. One common method of actuation is through electroosmotic flow (EOF) which involves the movement of ions in a solvent as a result of an applied potential. EOF can be used to affect the working fluid directly, or to induce a hydraulic flow which in turn works pumps and valves, or acts on the working fluid. Another means of actuation makes use of temperature dependent properties such as viscosity or the presence of bubbles. In one example, a sample stream flowing through a Y-shaped channel was controlled by thermally changing the viscosity of two streams flowing along either side of the sample stream. In others, thermally induced bubbles have been used to actuate gates, pump fluid along a channel, or to mix fluids or generate pressure through bubble expansion and compression. Another means to control flow is through the use of capillary pressure, which has been used to move fluids along channels or has been set opposite other forces to act as a means of gating. Further examples of active elements have made use of materials that change volume and shape based on pH, hydrophobic regions of channels that prevent fluid from flowing past, Lorentz forces to move fluid, ferrofluidic plugs actuated by magnetic forces, and piezoelectrically actuated pumps. [2]

Of the wide variety of microvalves and pumps described, many incorporate moving parts that require flexible materials. One fairly straightforward mechanical valve that requires flexible materials can be seen in figure 1-2.

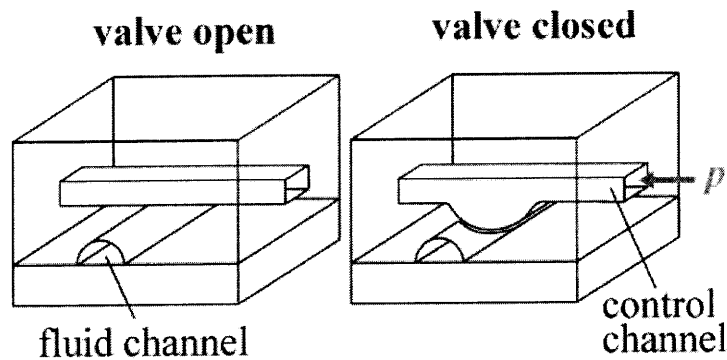


Figure 1-2 A simple valve that uses pressurized expansion of a control channel to seal a fluid duct [6]

This valve system consists of two layers of channels. The lower layer contains fluidic ducts for the sample fluid, while the upper layer holds pneumatic control channels. In places where the ducts and pneumatic control channels cross, a pressure applied to the control channel will cause it to expand down into the fluid channel, as can be seen in the image on the right side of figure 1-2. The expanded control channel blocks the fluid flow in the duct, closing the valve [6]. Despite their simple design, valves such as these can be useful in a variety of applications. For example, by locating a valve on each side of a T-shaped channel, it is possible to create a fluidic switch that directs flow down a specified path. It is also possible to use several valves actuated in series to create a pump (figure 1-3(b)), or, if the pumped fluid is circulated within a loop, a mixer (figure 1-3 (c)) [6].

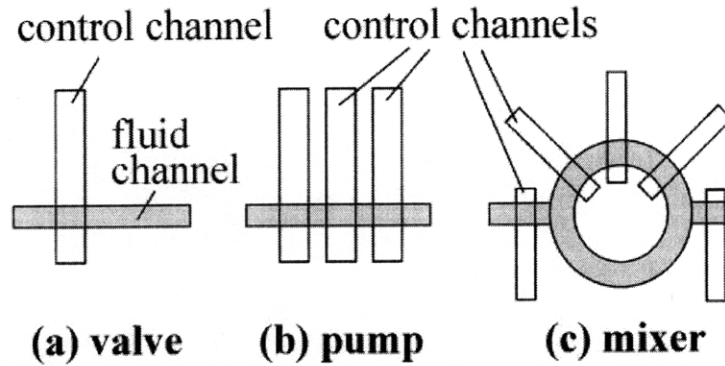


Figure 1-3 The valve from figure 1-2 arranged to function as a simple valve (a), in series to create a pump (b), and in series on a closed loop to create a mixer (c) [6]

The same type of valve was also used by Thorson et.al. to create their LSI comparator chip, shown in figure 1-3. By arranging valves in a binary tree composed of multiplexors, Thorson et.al. were able to control n fluid channels using only $2\log_2 n$ control channels [3].

1.2.2 Material Selection

To create valves such as those described in the previous section, a flexible material is needed. Thus far, polydimethylsiloxane (PDMS) has been a common choice for fabricating flexible active elements for microfluidic devices. PDMS parts are easily fabricated using soft lithography, a process which involves combining a base and a curing agent to form liquid pre-polymer, then pouring this pre-polymer over a master mold and allowing it to cure. Mold features can be closely replicated using this method with high fidelity, in the range of 10's of nm [7]. Other advantages of the soft lithography fabrication process include the fact that it allows for rapid prototyping, does not require expensive capital equipment, and has tolerant process parameters that allow production outside of clean rooms [8]. One potential disadvantage of molding PDMS using soft lithography is that the process cannot be directly used to fabricate 3D structures. As it is

difficult to create moving parts with only a single layer of PDMS, a multilayer technique wherein several layers of PDMS are stacked on top of one another and bonded together has been employed [7, 8]. PDMS can be bonded either reversibly, through van der Waals forces or adhesive tapes, or irreversibly, through oxidative sealing or by creating layers with an excess of either base or curing agent, placing opposing layers together, and curing them [7, 8]. Using the second of these techniques, Unger et.al. have fabricated devices with as many as seven layers, as well as pumps and valves [8].

However, fabricating microfluidic devices using PDMS is not without problems. For one thing, because PDMS is a combination of two components, a base and a curing agent, batch differences due to slightly different ratios can lead to inconsistent end results. Furthermore, fabricating devices from PDMS using soft lithography can take much longer than using thermoplastic materials that can be processed using more traditional methods, such as injection molding or hot embossing. Cure times of several hours significantly increase the time needed to fabricate parts from PDMS, while hot embossing requires on the order of 5-7 minutes per part, and injection molding requires on the order of only 1-3 minutes per part [9]. In any high volume production scheme, in which rate will become important, the long curing times of PDMS would be undesirable.

Thermoplastic elastomers (TPEs) provide an alternative to PDMS for the fabrication of flexible devices. TPEs are two phase materials that soften upon heating and can be processed using the same methods used for standard thermoplastics, including injection molding and hot embossing [10, 11]. By taking advantage of these faster processing techniques, fabrication of parts from TPEs can yield faster production rates than fabrication from PDMS [9]. Upon cooling after processing, TPEs take on rubber-

like qualities, and can demonstrate flexibility similar to that of PDMS, as shown in table 2-1 [10, 11]. This flexibility makes them suitable for fabrication of active elements that require moving parts, such as the valves described earlier in this section. In addition, TPEs demonstrate a wide range of properties, and may be suitable in applications for which PDMS cannot be used [10, 11]. Given the production benefits of thermoplastic alternatives to PDMS, it is worthwhile to investigate the use of TPEs for producing microfluidic devices.

1.3 Thesis Overview

This investigation seeks to determine the feasibility using hot embossing to fabricate microfluidic devices from TPEs. Specifically, it seeks to characterize the processing window of a single TPE in order to provide guidance on optimal processing conditions for fabricating microfluidic devices and to establish a method for characterizing process windows of TPEs in general. Chapter 2 provides background information about the properties of TPEs and describes the selection process of the particular TPE as well as the hot micro-embossing (HME) process. Chapter 3 discusses the specific experimental setup and procedures, and describes the process used to take measurements and process data. Chapter 4 seeks to analyze and interpret the results obtained during the course of the investigation. Finally, Chapter 5 summarizes the results, draws conclusions, and makes suggestion for future investigations.

2 Background

2.1 Thermoplastic Elastomers

2.1.1 Overview of Thermoplastic Elastomers

Thermoplastic elastomers (TPEs) are a type of polymeric material that combine a polymer with thermoplastic qualities and one with rubber-like behavior, typically through physical, thermoreversible crosslinks. Most TPEs, with the exception of melt processible rubbers and ionomer-based materials, take the form of two phase systems. One of the phases is hard at room temperature, giving the material its strength and preventing it from flowing. The other is a soft, rubbery elastomer at room temperature and provides the TPE with flexibility. The hard phase provides physical crosslinking for the polymer network, similar to the way that chemical crosslinking provides structure for vulcanized rubbers, as seen in figure 2-1.

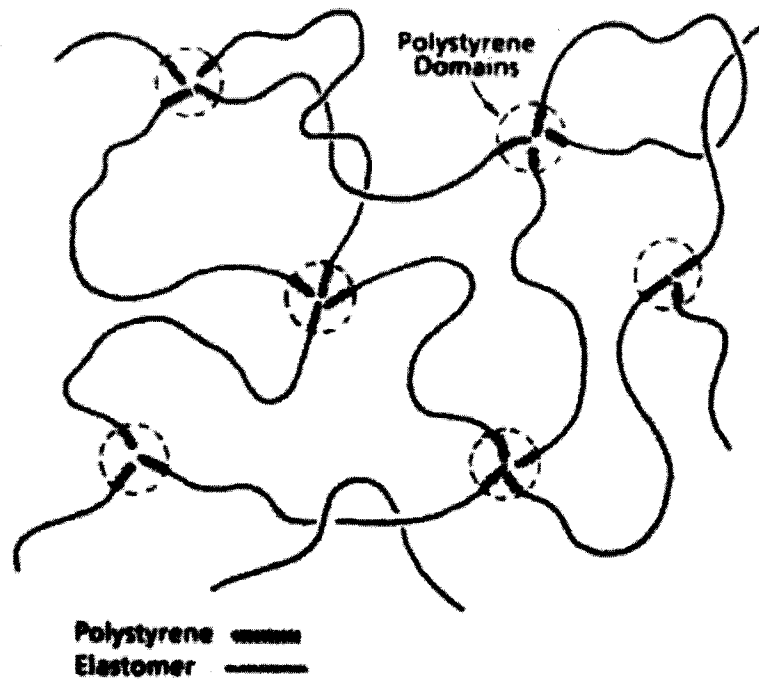


Figure 2-1A TPE with a polystyrenic hard phase. The polystyrene domains act as crosslinks for the elastomer. [10]

The difference is that the physical crosslinks of TPEs, unlike the chemical crosslinks of traditional rubbers, are not permanent and lose their strength when subjected to temperatures above the glass transition or melt temperature of the hard phase. The result is that TPEs can be subjected to temperatures high enough to disrupt the crosslinking and processed as though they were thermoplastic, then cooled, causing the crosslinks to reform and the TPE to behave as a flexible rubber once more. [10-12].

2.1.2 Previous use of TPEs for Microfluidic Applications

Stoyanov et.al. have used double sided hot embossing of TPEs to fabricate microfluidic devices for an analytical biosensor system with integrated valves. The selection of a TPE, specifically Walopor 2201 AU, a thermoplastic polyurethane foil, was based upon the need for chemical resistance against biological solutions, good elasticity

and sealing properties, low price, the potential for batch production, and transparency. The hot embossing process used tools made of milled brass with 100 μ m features, an embossing pressure of 5MPa, a temperature range was 140C-148C, and allowed for alignment for the two halves of the double sided hot embossing machine within +/-3 μ m [13, 14]. The microfluidic device produced includes four channels for fluid flow, each of which has an active valve. Valves were fabricated by creating reservoirs on the channels during the hot embossing step, which were later filled with PDMS. A TPE cover foil of the same material as the chip itself was then chemically bonded to the surface of the chip. Where the reservoirs filled with PDMS contacted the cover foil, bonding did not occur, allowing the cover foil to act as a membrane for the valves. Actuation of the valves is pneumatic, making use of pressurized air to limit deflection the membrane, effectively closing the valve. When the pressurized air is turned off, opening the valve, the membrane expands outward under the pressure of the fluid in the channel, allowing flow to pass. The integration of valves has limited the amount of sample fluid used and reduced fluidic exchange times to the order of 6-8 seconds [13]. The microfluidic system developed by Stoyanov et.al. has been used to successfully perform surface acoustic wave (SAW) analysis of the binding between thrombin and it's antibody [13, 14].

2.1.3 TPE Selection for the Current Investigation

The topic of the current investigation is the use of hot embossing to fabricate microfluidic devices from TPEs. Specifically, this study seeks to select a single TPE that seems well suiting to fabricating microfluidic devices and to develop a processing window for hot embossing this TPE. Several factors were considered during the material selection process. One important factor considered was elasticity. This investigation

seeks to develop TPEs as a potential alternative to PDMS, with a particular emphasis on flexible active elements. PDMS has a low elastic modulus, on the order of 1-2MPa, making it well suited for fabricating flexible elements, so the TPE selected would ideally have an elastic modulus on this same order. A low elastic modulus also further differentiates the hot embossing processing window of the TPE selected from that of the hard polymers previously embossed using the current system. This provides a lower bound for the elasticity processed by the current system, providing greater insight than would a less flexible material. Another consideration was whether the processing temperature of the material was within the range of the available hot embossing machine. Although the current machine can reach temperatures of up to 175°C, the higher temperatures require longer processing times, and a lower processing temperature, in the range of 90-120°C is desirable. Additionally, in order to be hot embossed, the material selected must be available as sheet or film with a thickness between 0.5-4mm. Furthermore, it is preferable that the material selected be biocompatible and transparent, such that it is suitable for biological and optical applications. Finally, the current investigation is on the research scale and uses only a small amount of material for each experiment. Thus, from a practical point of view, it would be best to select a material that can be purchased in small quantities, or even one for which an acceptable amount is available as a sample.

A variety of TPEs that approximately met the above specifications was investigated. Table 2-1 provides information on some of the properties of the TPEs considered. It should be noted that the information available on the properties of various TPEs is inconsistent, and the table reflects this. The categories selected for comparison

represent those that were relevant, and for which information was available for the majority of materials. For the category of processing temperature, it should be noted that due to inconsistent information, the temperatures provided represent a number of different values, including service temperature, Vicat softening point, and melt temperature. As such, they offer only an approximate idea of processing temperature and cannot be compared directly.

Material	Modulus at 100% strain (MPa)	Elongation at Break (%)	Processing Temperature (°C)	Transparency
Dow Sylard 184 (PDMS) [15]	1.8MPa [16]	160% [16]	RT-150°C	Excellent
Stevens Urethane ST-1880 [17]	6.89 MPa	450%	-51°C to 93°C (Continuous service temp.); 171°C to 193°C (melting point)	Excellent
Noveon Estane 58134 [18]	7 MPa	530%	94°C (Vicat softening point)	Excellent/Good [19]
Noveon Tecoflex EG 80-[20]	6.89 MPa	660%	154°C to 193°C (injection molding temp.); 182°C (melting point)	Excellent
Dow Pellethane 2355-80AE [22]	6.2 MPa	550%	93°C (Vicat softening point); 193°C (melt for molding)	Excellent/Good
SK Chemicals Skythane S175A [22]	3.59 MPa	940%	84°C (Vicat softening point); 190°C (melting point)	Good (maybe Excellent)
DSM Arnitel EM 400[23]	50 MPa	300%	195°C (melting point); 140°C (vicat softening point)	Fair
Arkema Pebax 4033 [24]	77 MPa	450%	131°C-160°C	Excellent/Good

Figure 2-2 A table comparing the properties of PDMS and a number of TPEs.

The first material on figure 2-2, separated from the others by a dashed line, represents the material properties for PDMS, which acts as a benchmark against which the TPEs can be compared. Of these TPEs most, with the exception perhaps of DSM's Arnitel and Arkema's Pebax, which have high elastic moduli, would have been fairly well suited to

the investigation at hand. However, of the materials, the Stevens Urethane 1880 was available in sheets, while several other were sold only in pellet form, and the company was willing to provide a free sample of more than adequate size. Thus, the current investigation focuses on Stevens Urethane 1880, although researching other potentially suitable materials is a promising area of future study.

2.2 Hot Micro-embossing

2.2.1 Overview of HME

One means of fabricating microfluidic devices from TPEs is hot micro-embossing (HME). The HME process involves heating a polymer above its glass transition temperature to soften it, then imprinting it using a tool. The polymer deforms viscoplastically into the mold, replicating the negative of the mold's microstructures [25, 26, 27]. The process steps of HME can be seen in figure 2-3.

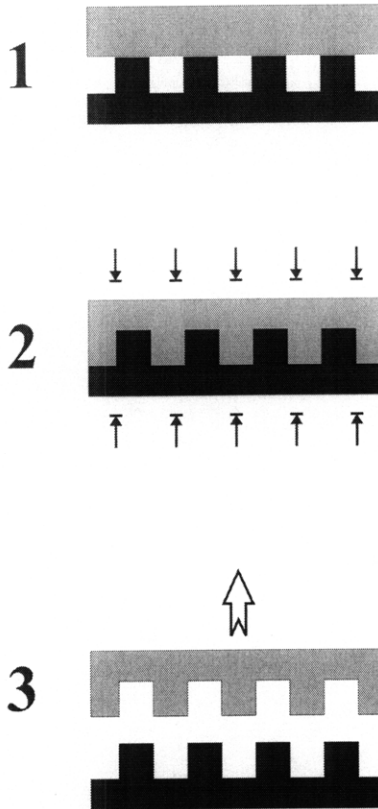


Figure 2-3 Processing steps for hot micro-embossing. The polymer workpiece is shown in gray, while the micromachined tool is black [26]

In step one, the polymer workpiece is inserted into the embossing machine and both the workpiece and the micromachined tool are heated from ambient temperature to the embossing temperature, which is set somewhere above the glass transition temperature of the polymer. In step two, an embossing force is applied, causing the workpiece to deform and fill in the microstructures of the tool. The workpiece and tool are held constant at the embossing temperature and force for some period of time, allowing the polymer to fully replicate the features of the tool. Then, in step three, the embossing force is held as the workpiece and tool are cooled to the deembossing temperature, at which point the force is released and the workpiece and tool are separated [26, 27]. Figure 2-4 shows the temperature and force trajectories during steps of the embossing process.

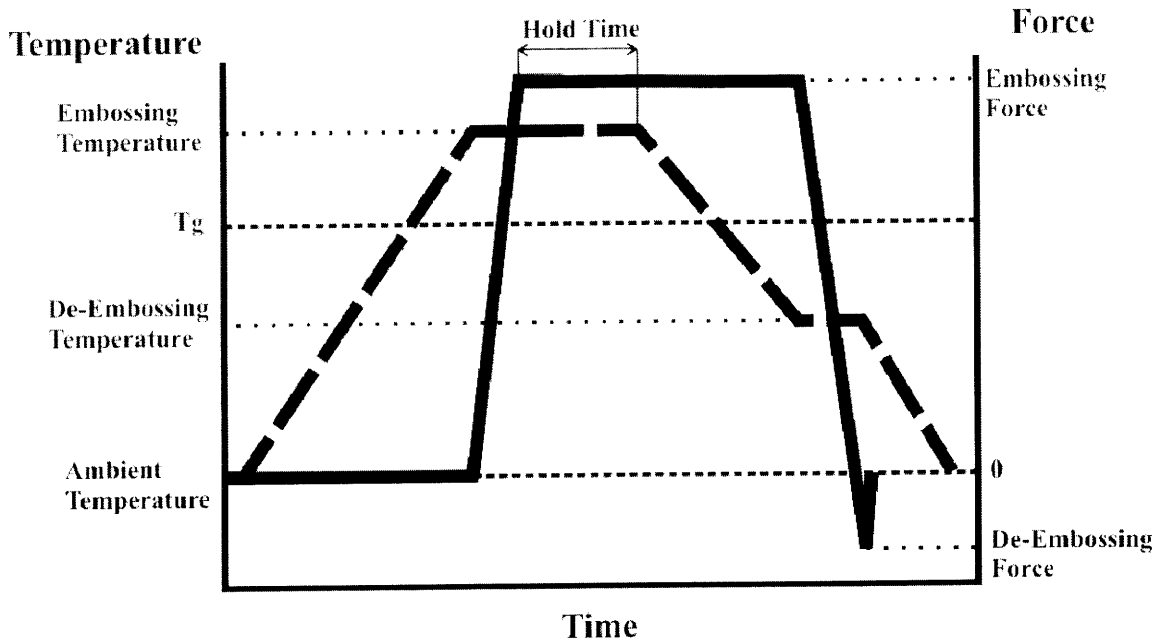


Figure 2-4 Temperature and force trajectory during HME. Force is shown by the solid line and temperature is shown by the dashed line. [26]

The negative force seen in figure 2-4 at the end of the embossing process represents the force necessary to remove the workpiece from the tool. This force varies based on factors such as feature depth and complexity, and can be reduced by an anti-adhesion layer on the tool [26].

2.2.2 Past Examples of HME

HME has already proven to be an effective means to replicate microstructures on traditional thermoplastics [25, 26]. An advantage of hot embossing is the short distance traveled by the polymer into the microstructure, which results in less residual stress, making hot embossed parts well suited for optical applications. The reduction in bulk material flow can also lead to less shrinkage and reduce friction during de-molding, thus making it possible to fabricate parts with higher aspect ratios [26, 27]. Despite the success with tradition thermoplastics, research on hot embossing TPEs is somewhat limited. One example of hot embossing TPEs has been presented by Styanov et.al. in

their investigation of TPE microfluidic chips for SAW analysis, discussed earlier in this report. However, although Stoyanov et.al showed that it is possible to successfully hot emboss a TPE, they made no attempt to report quantitatively on the success of their hot embossing process [13, 14]. For traditional thermoplastics, qualitative analysis of hot embossing and the relationship between processing conditions and the quality of the end result has been more thoroughly investigated [25]. A study by Roos et.al. found that temperature and hold time are the most critical parameters for hot embossing thermoplastics, specifically PMMA, while pressure needs to be above a certain value, but has less of an impact than the other parameters [28]. In an investigation to determine the ideal processing window for PMMA, Wang found a similar threshold effect for pressure, below which filling of the mold would be incomplete. Wang reported the ideal embossing temperature to be just above T_g , with higher temperatures resulting in a decrease in channel fidelity and an increase in variance. The de-embossing temperature was found to have an upper bound, above which part quality decreased [25]. While these findings may not hold true for hot embossing TPEs they do provide a basis for comparison, as well as some insight into the embossing process in general.

3 Experimental Method

3.1 HME Machine

The HME system used for this investigation was designed by Matthew Dirckx, a graduate student under Professor David Hardt of MIT, as the subject of his Master's thesis [26]. The HME machine can be seen in figure 3-1.

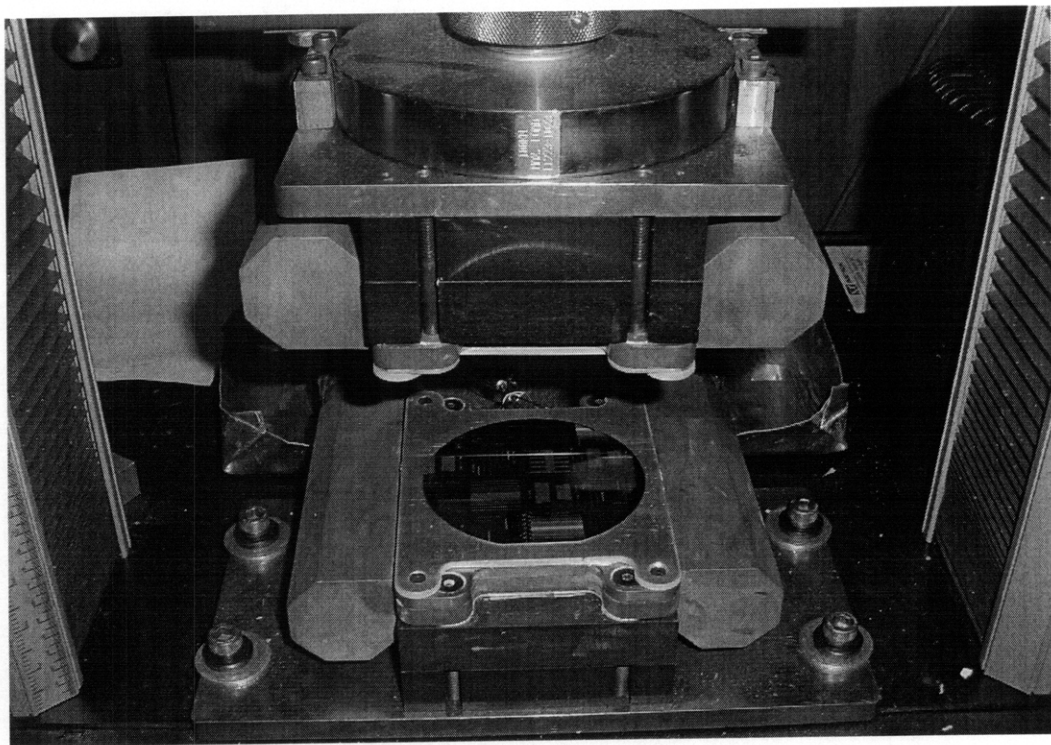


Figure 3-1 HME machine

In this HME machine, the embossing pressure is applied by an Instron model 5869 electromechanical load frame. The Instron can produce forces of up to 50 kN and can be controlled based on either force or displacement using a number of waveforms or user generated trajectories. For heating and cooling, the load frame is fitted with two copper platens, the temperature of which is controlled by a hot oil heating system. Temperature

control is based on a separated stream system in which a hot oil stream and a cold oil stream are mixed to attain oil of the desired temperature. Until mixing, the streams are separate, the hot side heated by an electric joule heater and the cold side cooled by a plate and frame heat exchanger with a continuous stream of tap water as the cooling fluid. The mixing valves are automated, and the operator can either set the mixing ratio of hot to cold oil to control temperature for each of the platens individually. Alternatively, the temperature control system can carry out pre-programmed temperature profiles. This level of automation allows for repeatability and eliminates some potential errors inherent to a manually controlled system. The oil used for the system is Paratherm MR, a paraffinic hydrocarbon oil, has a boiling point of above 300°C, although the system was only designed to reach temperatures of 175°C. [26] For the maximum temperature investigated, 150°C, the HME machine took about 6 minutes to reach temperature, and about 5 minutes to cool to 50°C.

3.2 Mold

The tool used for hot embossing was originally designed to fabricate parts for polymerase chain reaction (PCR) by Vikas Srivastava, a PhD student in Mechanical Engineering at MIT [29]. A schematic image of the tool can be seen in figure 3-2 below.

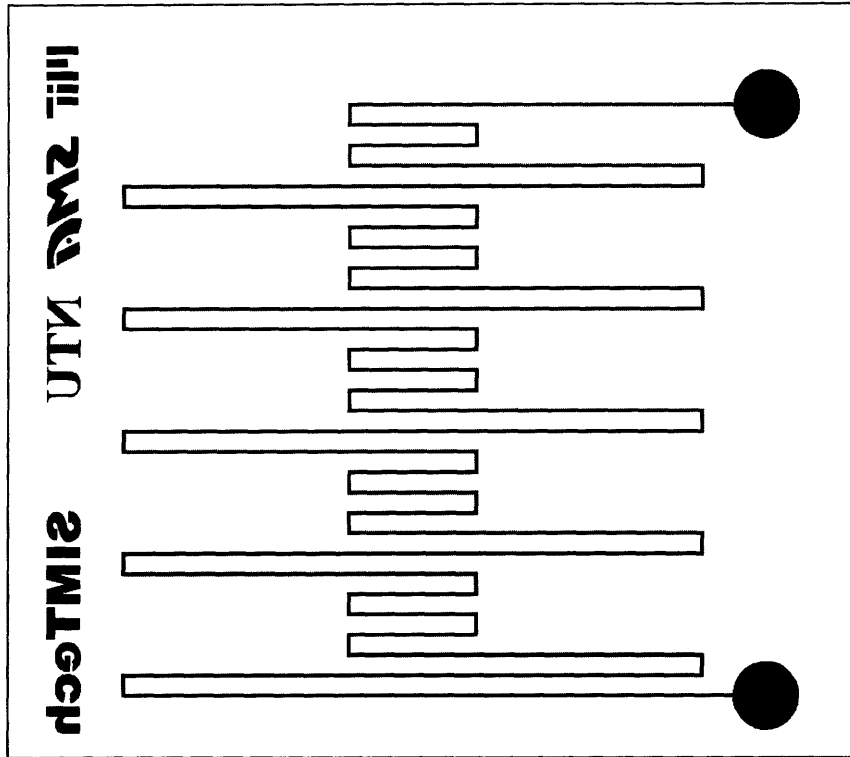


Figure 3-2 Schematic of the tool used for hot embossing.

As can be seen in figure 3-2, the tool is designed to fabricate parts with long winding channels. The raised channel microfeatures on the tool, measured using the optical profilometer discussed in section 3.4, extend a height of about $66\mu\text{m}$ above the surface of the tool and are measured to be about $80\mu\text{m}$ wide. The entire tool is about 1in^2 , and the features are offset slightly so they are closer to one edge, as seen in figure 3-3.

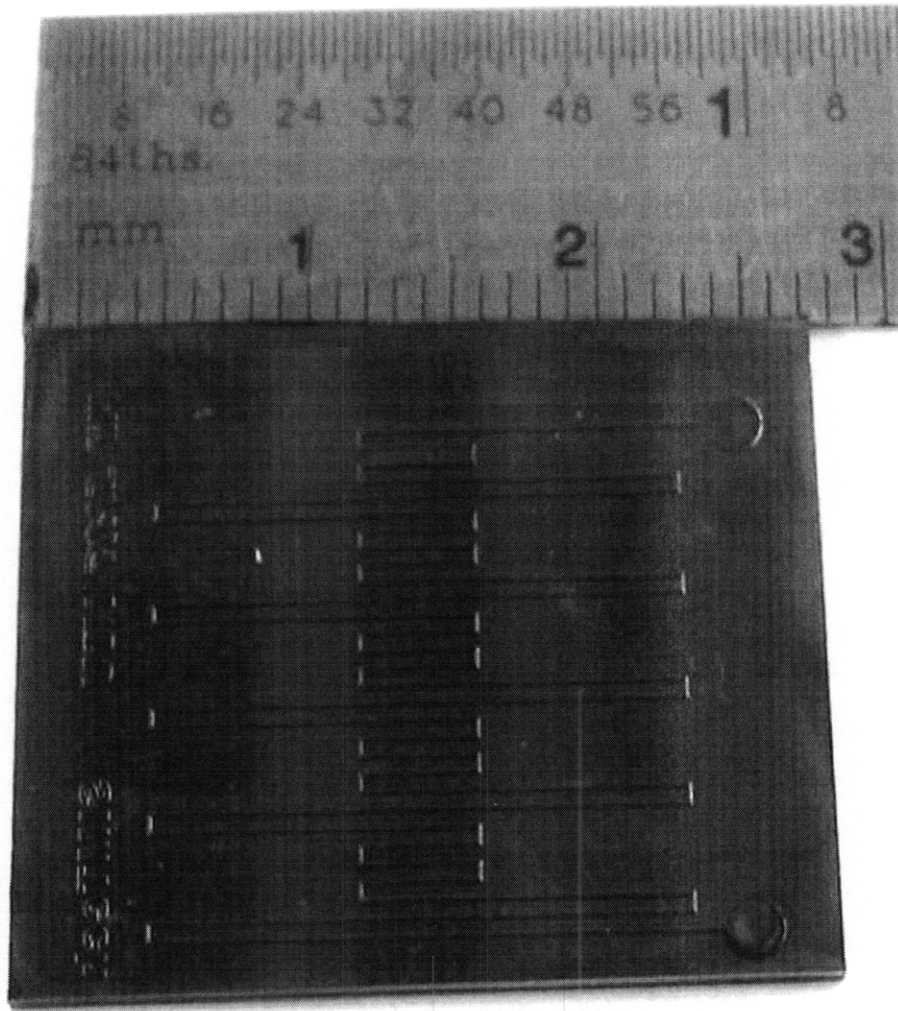


Figure 3-3 Photo of the tool, showing tool size.

The tool is fabricated from bulk metallic glass (BMG), a strong material that can hold up well under high embossing pressures or de-embossing forces [29]. A SEM of the tool showing a close up of features can be seen in figure 4-4. This tool was used for all parts embossed during this investigation.

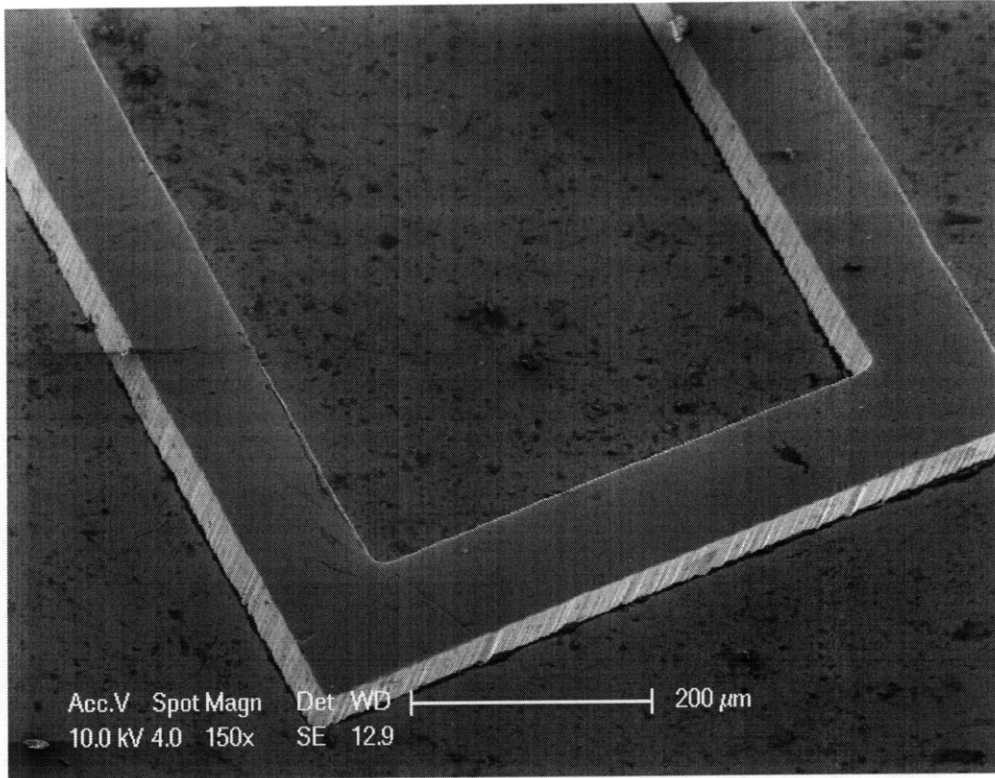


Figure 3-4 SEM image of the tool, showing a detailed view of tool features.

3.3 Procedure for Tests

Experiments were performed using approximately 1 in^2 , 1mm thick pieces of Stevens Urethane 1880. To run tests, the tool was placed on an aluminum plate, which was used to facilitate transport to and from the platens. A TPE workpiece was placed on top of the tool, and a piece of Teflon, intended to promote uniform pressure distribution across the part and prevent adhesion with the opposite platen, was placed on top of this. This setup can be seen in figure 3-5.

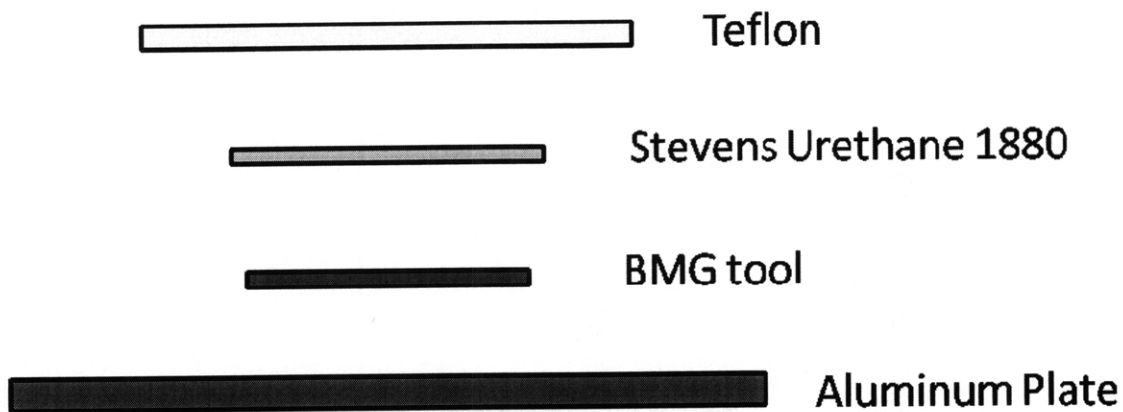


Figure 3-5 Schematic of the stack setup used for embossing.

The aluminum plate, tool, workpiece, and Teflon were all placed between the copper platens. The upper platen was lowered until it was touching the top of the Teflon, but not exerting a force, and the temperature of both platens was increased to the embossing temperature, which varied between experiments within the range of 100-150°C. Once at temperature, the platens were used to exert a pressure between 0.25-4MPa. The embossing temperature and pressure were held constant for one minute, and then the temperature was lowered to 50°C while the pressure was held constant. The de-embossing temperature of 50°C was chosen, based on experience, because at this temperature deformation after de-embossing is unlikely to occur, and because parts can be handled at this temperature. After the platens were cool, the upper platen was raised, and the aluminum plate setup was removed from the HME machine. The finished part was then peeled by hand from the tool.

3.4 Measurement and Data Processing

A Zygo NewView™ 5000 optical interferometer was used to measure the features of the hot embossed parts. Each part was measured in four locations, which can be seen in figure 3-6 below.

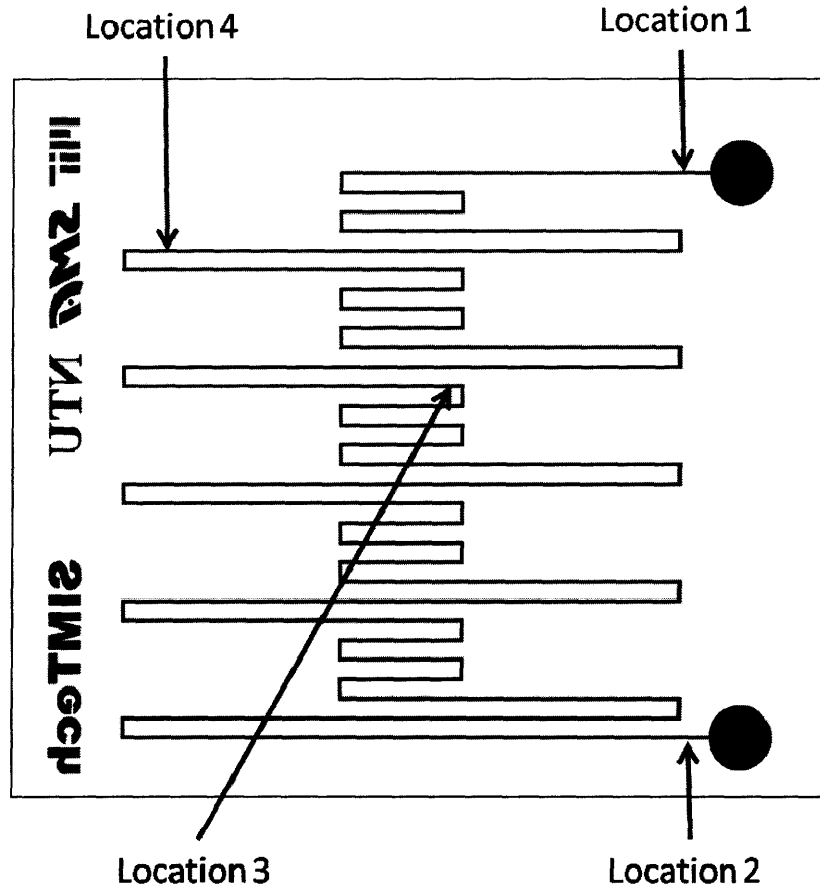


Figure 3-6 Schematic of the tool showing measurement locations.

Measurement locations were selected across the tool, including locations near the edges of the tool as well as near the center. These multiple locations can be used to verify across part uniformity, and determine trends based on tool geometry.

In order to process the data obtained on the Zygo, an open source program called Gwyddion was used. Gwyddion is designed to analyze and visualize data from scanning probe microscopy (SPM) and in this case was used to convert the height information

from the Zygo into 3D topographical images as well as cross sections. In addition, Gwyddion was used to correct the raw Zygo data. For areas where the Zygo failed to obtain data, such as sloped surfaces where the reflected light waves missed the detector, a Laplacian solver was used to fill in missing information. Using data surrounding the area to define boundary conditions, the solution to the Laplace equation was determined iteratively and substituted in for the missing data. For some of the data, Gwyddion's leveling function was used to correct for slant imposed by imperfect leveling when taking measurements. However, in some cases, slanted channel walls or rough surfaces caused the leveling function to work improperly, and in these cases, the data was left as measured. The decision to use the leveling function was made qualitatively on a case by case basis. Finally, for each data set, the minimum value measured was shifted to zero, making it easier to interpret and compare results.

Once the data was corrected, cross sections and topographical images were created. For cross sections, a representative cross sectional profile perpendicular to the channel was selected. This profile was assigned a thickness of 128 pixels, the maximum possible, and the resultant composite cross section was evaluated based on the original profile selected, as well as data to either side of the profile within the 128 pixel range. Gwyddion was then used to fit a negative step function to the profile, from which channel depth and width were determined. A typical Gwyddion window for the step function fit can be seen in figure 3-7.

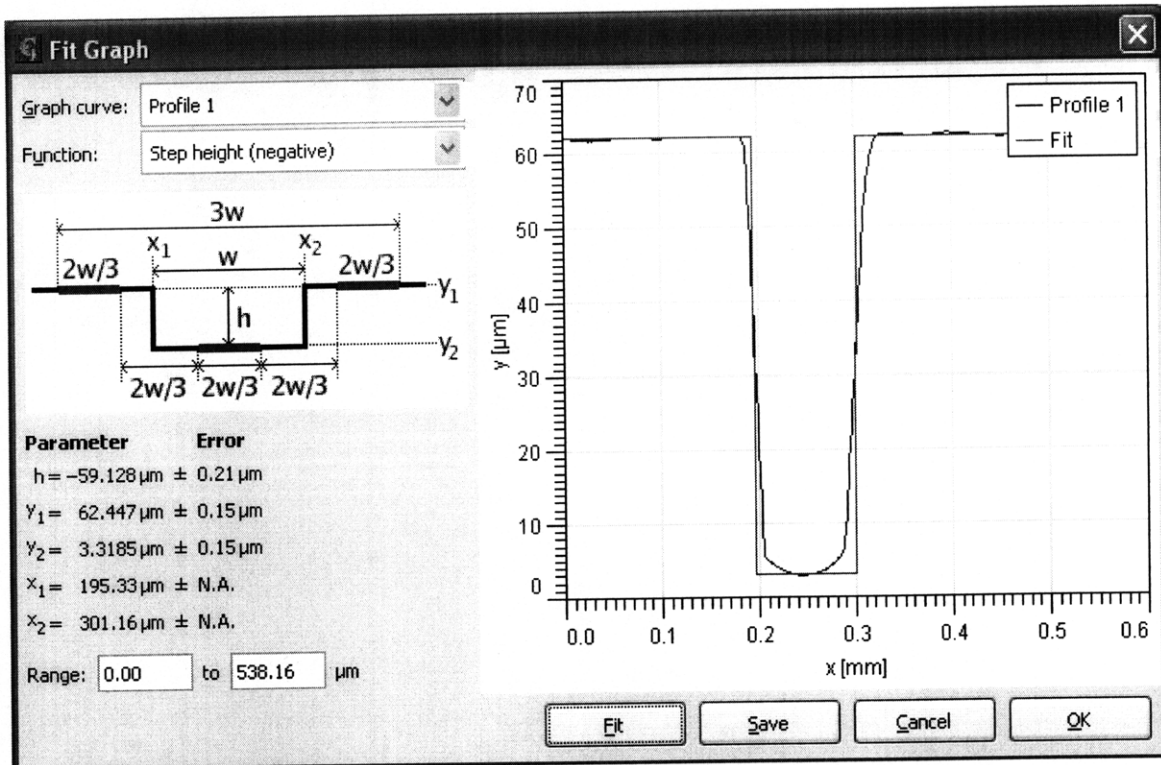


Figure 3-7 A Gwyddion window showing the typical step fitting function applied to a cross section.

As seen in figure 3-7, Gwyddion directly provides the height of the channel as the “h” parameter. The width was determined by finding the difference between the x values for the channel walls, the x_1 and x_2 parameters in figure 3-7. It should also be noted that in some cases the step function fit was imperfect due to sloping channel sides, as seen in figure 3-8.

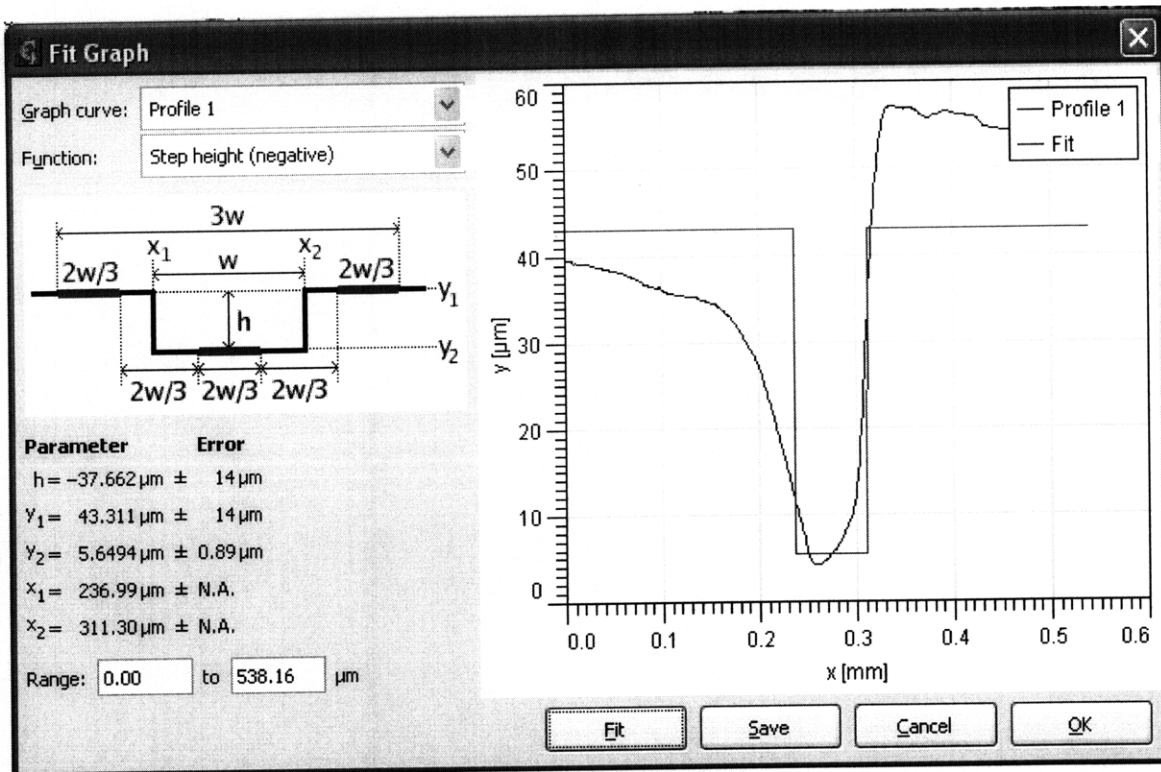


Figure 3-8 A Gwyddion window showing the step fitting function for an uneven profile.

In these cases, the channel depth and width provided by the solution of the step function are not necessarily accurate. Despite this, the best way to measure these quantities is uncertain and, to maintain consistency, the values returned by the step function were still used to determine channel depth and width.

In addition to cross sections, Gwyddion was also used to create 3D renderings of part topography. An example of such a rendering can be seen in figure 3-9.

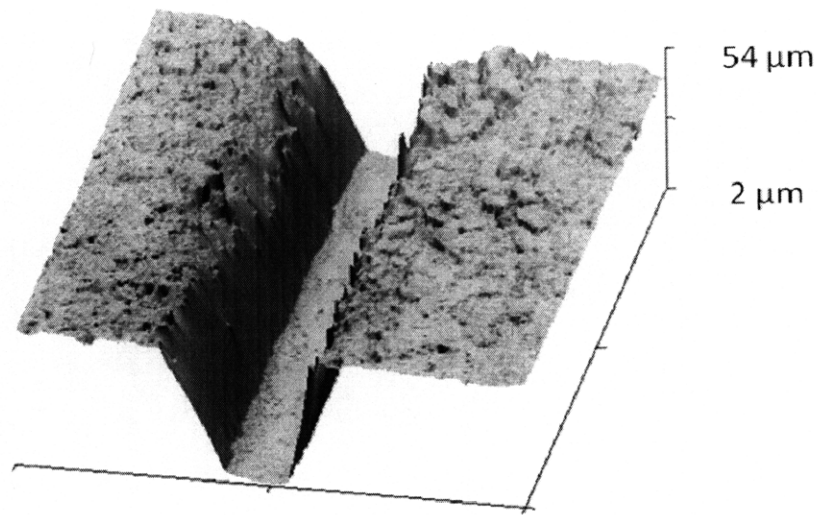


Figure 3-9 A Gwyddion 3D topography rendering of a part embossed at 130°C and 1MPa.

For this investigation, parts were rendered using Gwyddion's default Open GL material with lighting, although the program is also capable of using false color gradients. The topographical renderings of parts are helpful in visualizing the surface texture of parts as well as the shape of channels, as seen in figure 3-9. However, the appearance of feature depth is defined by the user, and does not necessarily give an accurate representation of the part. For example, in figure 3-9, the channel appears to be as deep as it is wide, when in reality it is shallower than it seems, about half as deep as it is wide. Despite this, the topographical renderings can provide useful information for interpreting results. [30]

4 Results and Discussion

4.1 Introduction

In this investigation, a specific TPE, Stevens Urethane 1880, has been successfully hot embossed. A variety of processing conditions have been studied, including temperatures ranging from 100-150°C and pressures from 0.25-4MPa. The success of each set of processing conditions, for the particular embossing tool and material used, was assessed based on the replication of channel width and depth relative to the original tool, as well as across-part uniformity. In addition, a smearing effect and residual surface roughness from the original surface of the un-embossed parts were observed but not quantitatively analyzed. From this data, a processing window for the particular conditions studied has been determined, and causes for the smearing effect have been hypothesized.

4.2 Criteria Used to Analyze Parts

For each of the four locations on the parts analyzed, cross sections were extracted using the procedure described in Chapter 3. A matrix of cross sections for each location based on the temperature and pressure used for embossing can be seen in Appendix A. The depth and width measured from the cross section for each location was then compared to the averaged height and width measurements of the part. For depth, channels within 10% of the height of the tool were considered well formed, channels within 15% of the tool height were considered borderline, and anything above 15% was

considered unfilled. For width, channels within 15% of the tool were considered well formed, those within 20% were considered borderline, and those above 20% were considered poorly formed. In order for an entire part to fall into one of these categories, three of the four locations had to fit the criteria. That is to say, for depth of an entire part to be considered well formed, for example, channel depth for three out of four channels must fall within 10% of the tool. Each part was further assessed for uniformity. Uniformity was determined by comparing the smallest value for depth or width from the largest. For depth, a difference of 5 μ m or below was considered uniform, and for width, a different of 15 μ m or below was considered uniform. If either height or depth is uniform, and the other is not, the part is considered borderline.

In order for an entire part to be considered good, all three criteria must be within the well formed range. If any of the criteria are unmet, depth difference greater than 15%, width difference greater than 20%, or non-uniform, then the part is not considered well formed. If one or two of the criteria fall within the borderline range, and the remaining criteria fall within the well formed range, the part is considered borderline. If any one of the three criteria falls outside the acceptable range, the entire part is considered inadequately formed. In addition, if a part displays bulk warping, that is to say that independently of channel measurements, the entire piece is curved or deformed in some way, it is considered poorly formed. An example of such a part can be seen in figure 4-1.

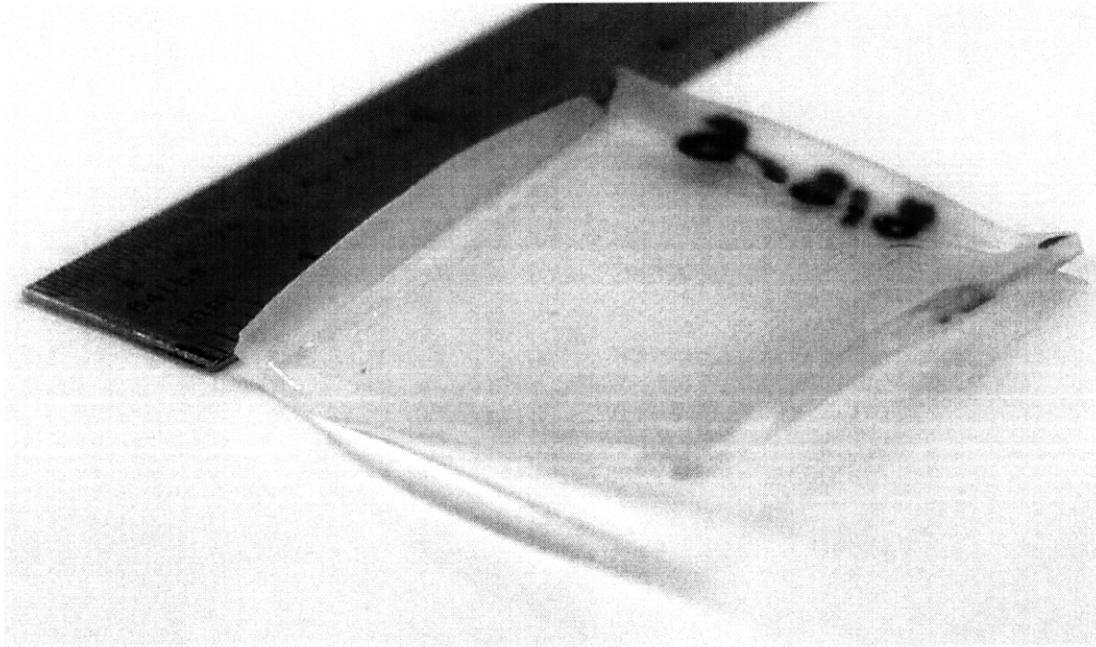


Figure 4-1 A part, embossed at 150°C and 2MPa, that displays bulk warping.

In some cases, specifically for the part shown in figure 4-1, which was embossed as processing conditions of 150°C and 2MPa, the part was not so deformed as to prevent measurement, and the channels on the part were found to be well formed.

4.3 Processing Window

The results of analyzing each part according to the criteria described above are seen in figure 4-2.

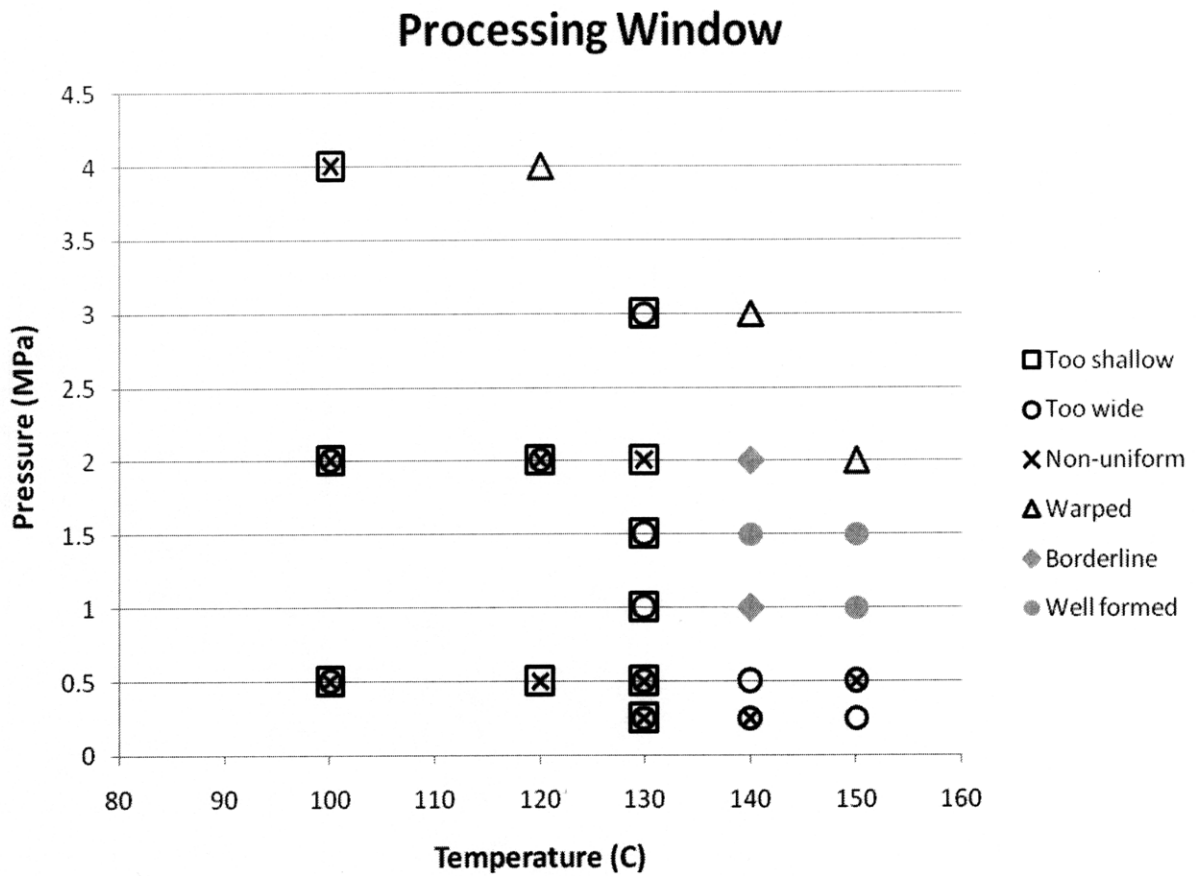


Figure 4-2 Processing window for Stevens Urethane 1880.

For each of the failed parts, symbols in figure 4-2 represent the reason the part was considered poorly formed. The symbols for borderline and well formed parts don't provide insight into each of the criteria, but more detailed information can be found in Appendix B. Another visualization of the processing window, specifically the depth results, can be seen in figure 4-3.

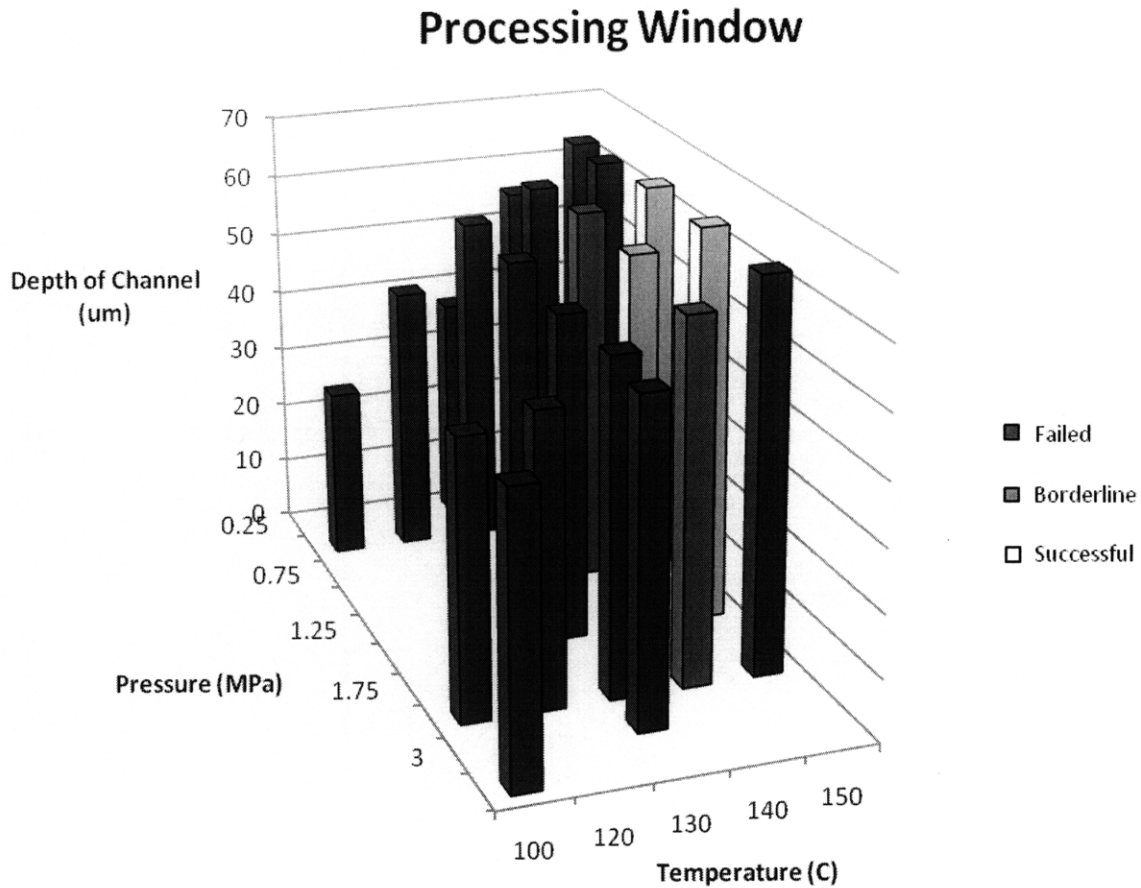


Figure 4-3 Processing window for Stevens Urethane 1880.

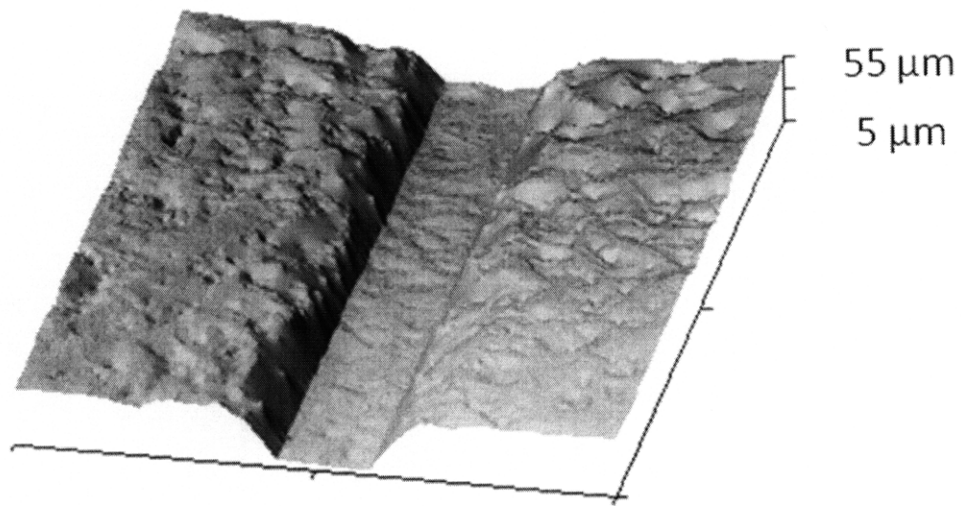
In figure 4-3, the floor of the graph conveys information about processing conditions, while the height of the bars corresponds to the average depth of the channels formed. The dark gray, light gray and white columns correspond to failed, borderline, and successful parts respectively, according to the above criteria.

From figures 4-2 and 4-3 it is evident that higher temperatures, 140°C and above, worked the best for channel formation. At lower temperatures, channels were consistently too shallow, while at temperatures of 140°C and above the channel depths were all within 15% of the height of the tool. Channel failure above 140°C was due to other problems, mostly issues with width, which were also less frequent than at lower

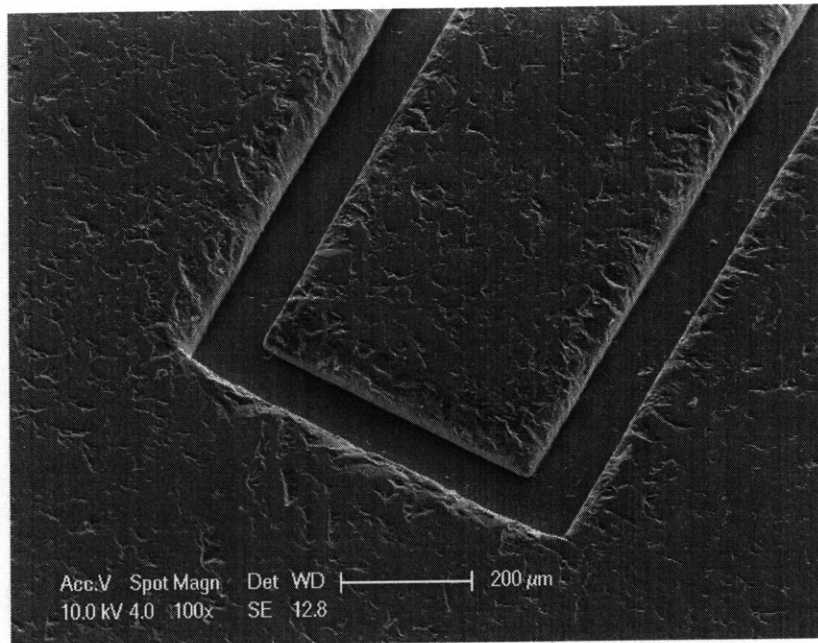
temperatures. Embossing at the highest temperature investigated, 150°C, was the most successful. Four of the five parts embossed at 150 °C had channel depths within 5% of the height of the tool. The most successful part was embossed at 150°C and 1.5 MPa, and demonstrated channel depths within 5% of the tool and widths within 10% of the tool for all four measurement locations, as well as good uniformity. There were also fewer problems with uniformity and width than for lower temperatures, especially at pressures above 0.5MPa. Indeed, the upper range of temperatures, which seems most promising, has not been fully explored, as no temperatures above 150°C were investigated.

However, the melt temperature of Stevens Urethane 1880 is cited by the company as around 170°C, and at temperatures approaching this, in the range of 150°C to 170°C the material is close to molten. Since hot embossing, by definition, takes place when a material is softened, but not molten, these higher temperatures may no longer be within the realm of hot embossing. This suggests that, although HME works to fabricate devices from TPE, a different process in which the material actually becomes molten, such as casting, may be more suitable.

In terms of pressure, the middle level pressures, in the range of 0.5MPa to 2 MPa resulted in good channel formation. At pressures lower than this, channel formation was incomplete, as evidenced by channels that are too shallow or wide and by residual rough surface textures from the original Urethane film, as seen in figure 4-4.



(a)



(b)

Figure 4-4(a) Gwyddion image of a channel embossed at 100°C and 0.25MPa. The channel is shallow and wide, and the surface is visibly rough. (b) SEM image of a channel embossed at 140°C and 1MPa. The residual surface texture from the TPE film is visible

The other end of the spectrum, pressures that are too high, results in bulk deformation of the part. This can be seen in figure 4-2, which indicates that at high enough pressures,

parts failed due to warping. The pressure at which parts begin to warp is temperature dependent, and at higher temperatures, it takes less pressure to cause a part to warp. This is the result of increased bulk material flow at higher temperatures, and is discussed in the next section. Similar temperature dependence can be observed at lower pressures, and at higher temperatures, lower pressures can produce more successfully embossed channels. It follows that at even higher temperatures than those used for this study, lower pressures could be used for embossing, while warping would take place more readily.

4.4 Channel Formation

Insight into the process of channel formation can be gained from superimposing cross sections taken at different conditions as seen in figure 4-5.

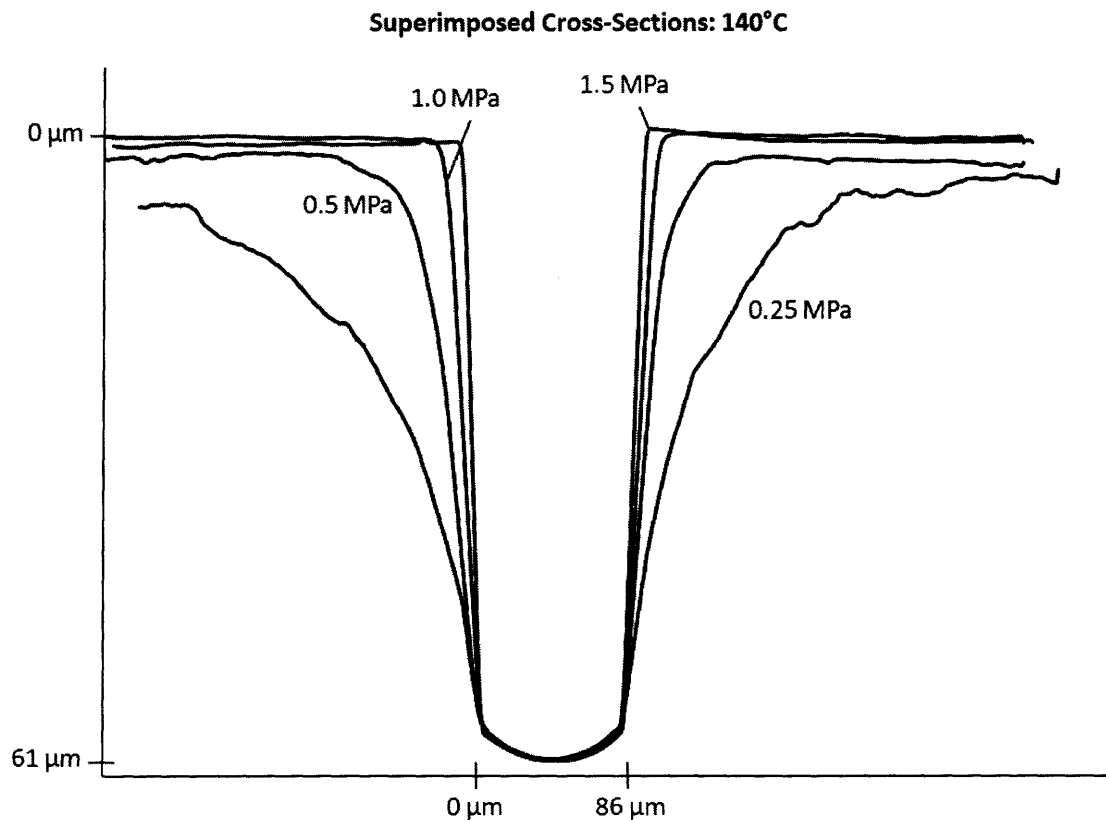


Figure 4-5 Superimposed cross-sections for parts embossed at 140°C and a variety of pressures.

As pressure is applied to emboss a part, it is increased over time and during the process the part is subjected to each of the pressures below the final embossing pressure.

Therefore, figure 4-5 can be viewed as a time progression of the HME process. When the tool first touches the part, it begins to depress the part where it is in direct contact, the highest part of the tool. Gradually, as more pressure is applied, the part material is forced into the tool features, contacting the side walls of the tool and then eventually filling in the corners for high enough pressures.

4.4.1 Smearing and Bulk Material Flow

Some of the embossed parts exhibit what appears to be smearing, especially for the measurement locations near the edge of the tool. This effect is sometimes so pronounced as to be visible with the naked eye, as seen in figure 4-6.

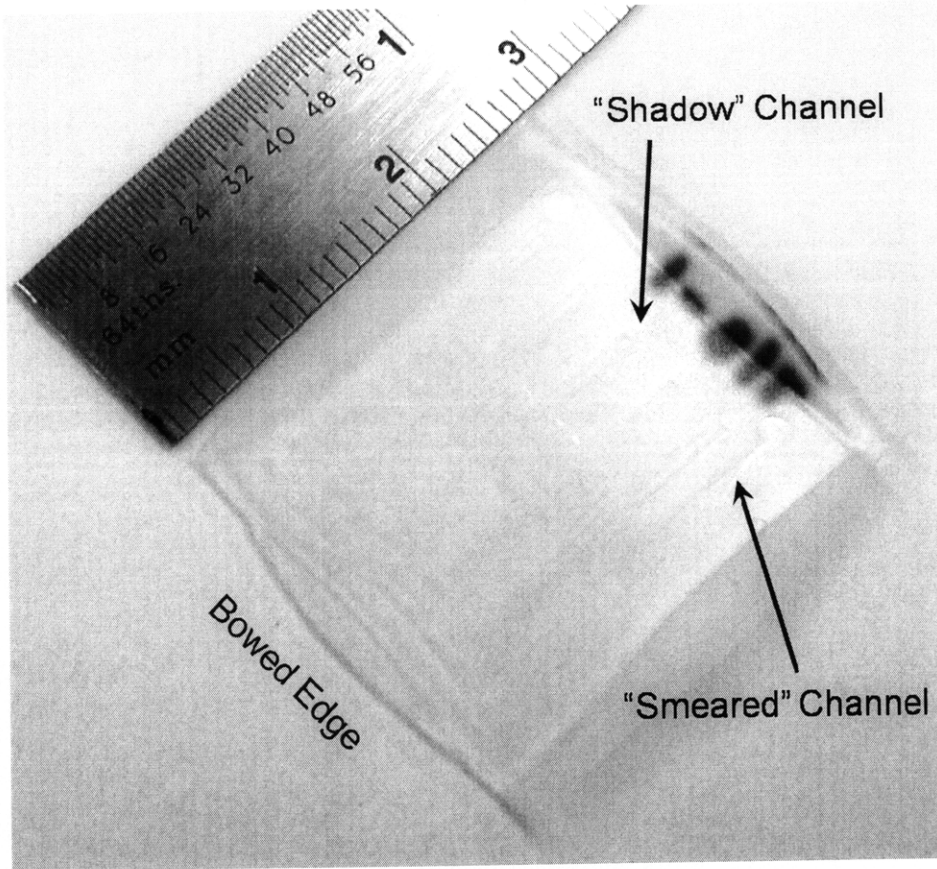
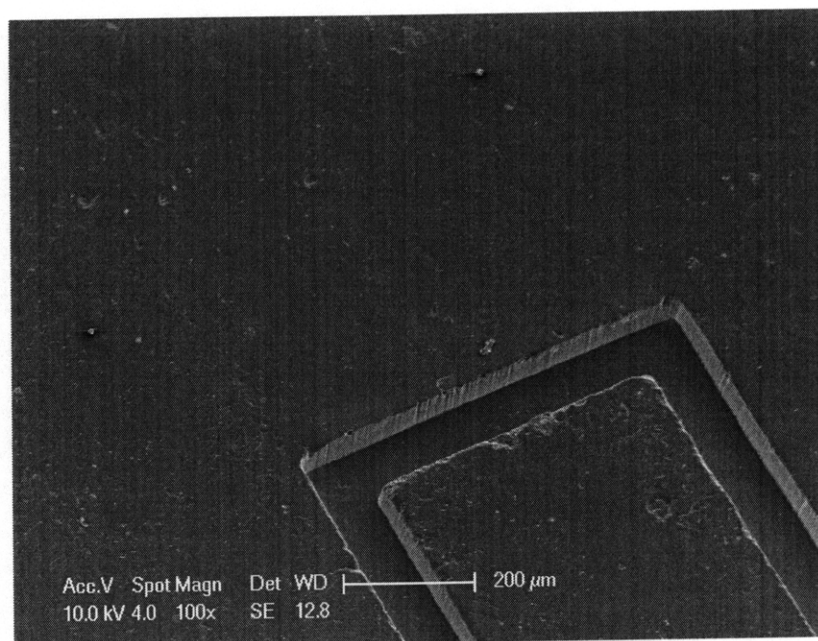


Figure 4-6 Photo of a part, embossed at 120°C and 4MPa, that demonstrates smearing. It is also particularly noticeable when comparing SEM images of smeared and un-smeared parts, as seen in figure 4-7.



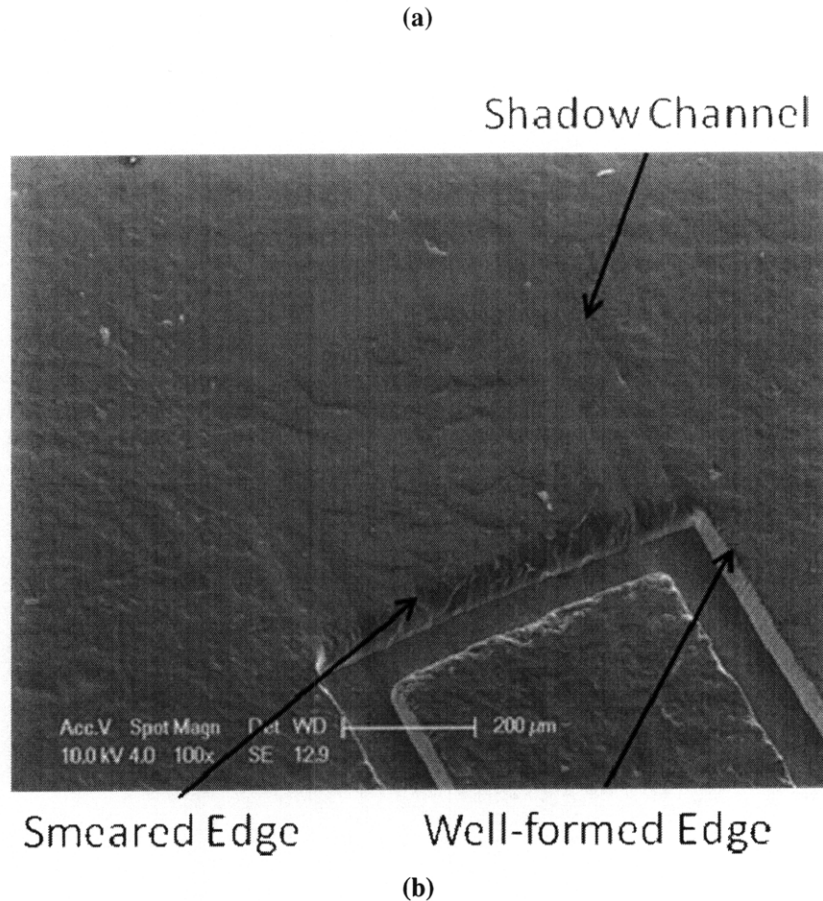
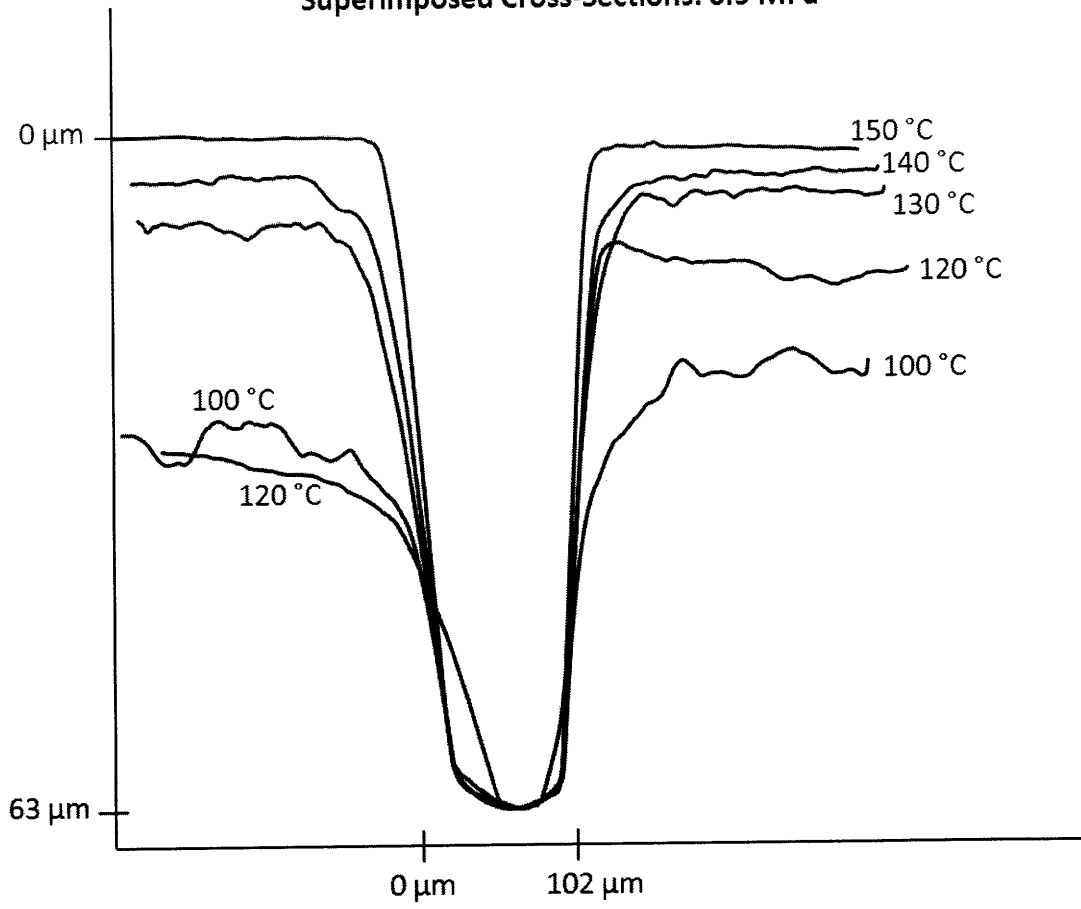


Figure 4-7 SEMs of the same location on two different parts. (a) A channel without smearing, embossed at 140°C and 1MPa. (b) A channel that shows smearing, embossed at 130°C and 1MPa

In figure 4-7(b) a shadow channel can be seen above the channel proper, as though the tool contacted the part and then slid along the surface before forming the deeper channel. The outer edge of the channel in figure 4-7(b), indicated on the image as the “Smearred Edge” is also noticeably sloped compared to the sharp edge of figure 4-7(a). However, there is a well formed edge visible in figure 4-7(b), the “Well-formed Edge,” explained later in this section by bulk material flow. The smearing effect can also be seen by superimposing cross sections, seen in figure 4-8.

Superimposed Cross-Sections: 0.5 MPa



(a)

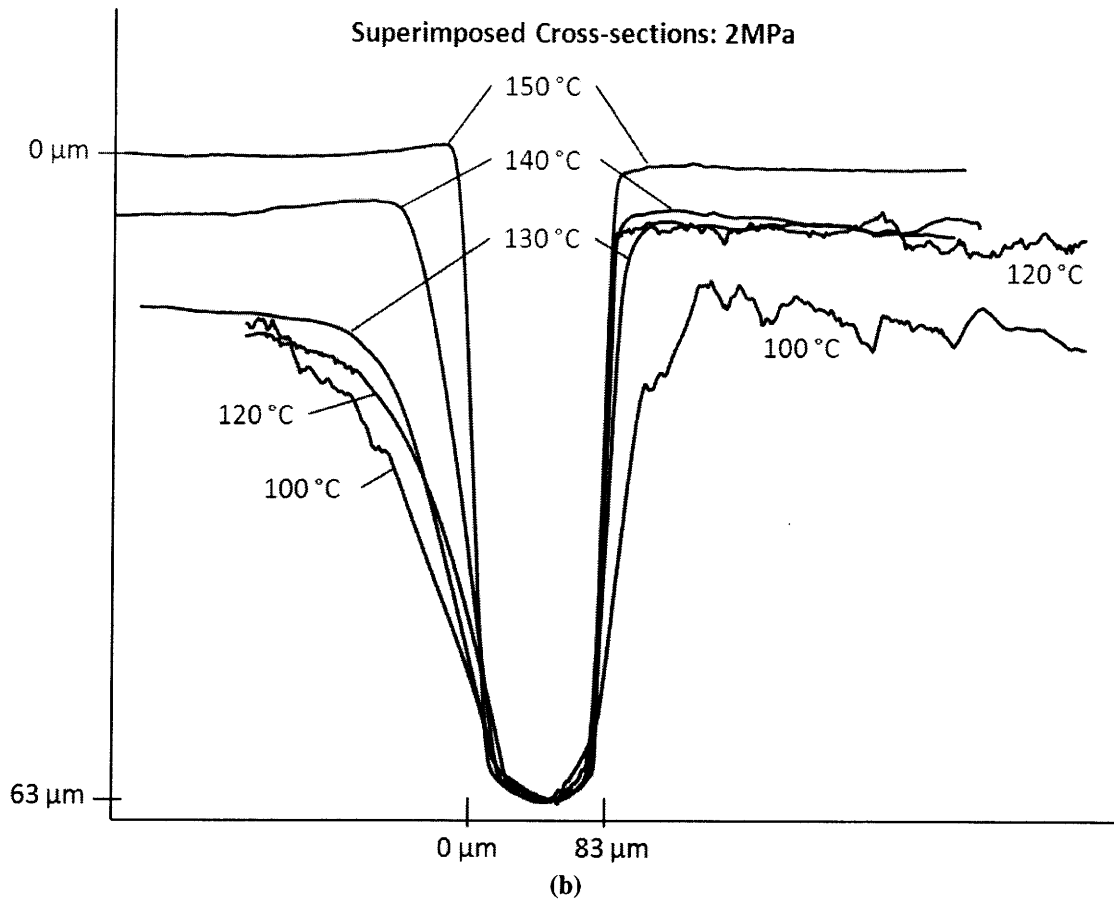


Figure 4-8 Superimposed cross-sections for parts embossed at 0.5 MPa (a), 2MPa (b), and a variety of temperatures.

From figure 4-8, it is evident that for parts embossed at lower temperatures, the upper portion of the channel on the left side is lower than those on the right, evidence of the smearing effect. For higher temperatures, this effect is reduced, although the walls on the left side are still more sloped than those on the right. Smearing also seems to be temperature dependent, as channels embossed at higher temperatures demonstrated less smearing than those embossed at lower temperatures. For greater pressures, the temperature threshold at which smearing is reduced appear to be higher, as parts embossed at 130°C and 2MPa were noticeably more smeared than those embossed at 130°C and 1.5MPa

The smearing effect observed can be explained by bulk material flow. When pressure is applied to the part, material flows not only into the tool features but also radially outward. For areas of the tool where the channel edge is towards the outside of the part, this bulk flow counteracts the flow of material into tool features, as seen in figure 4-9.

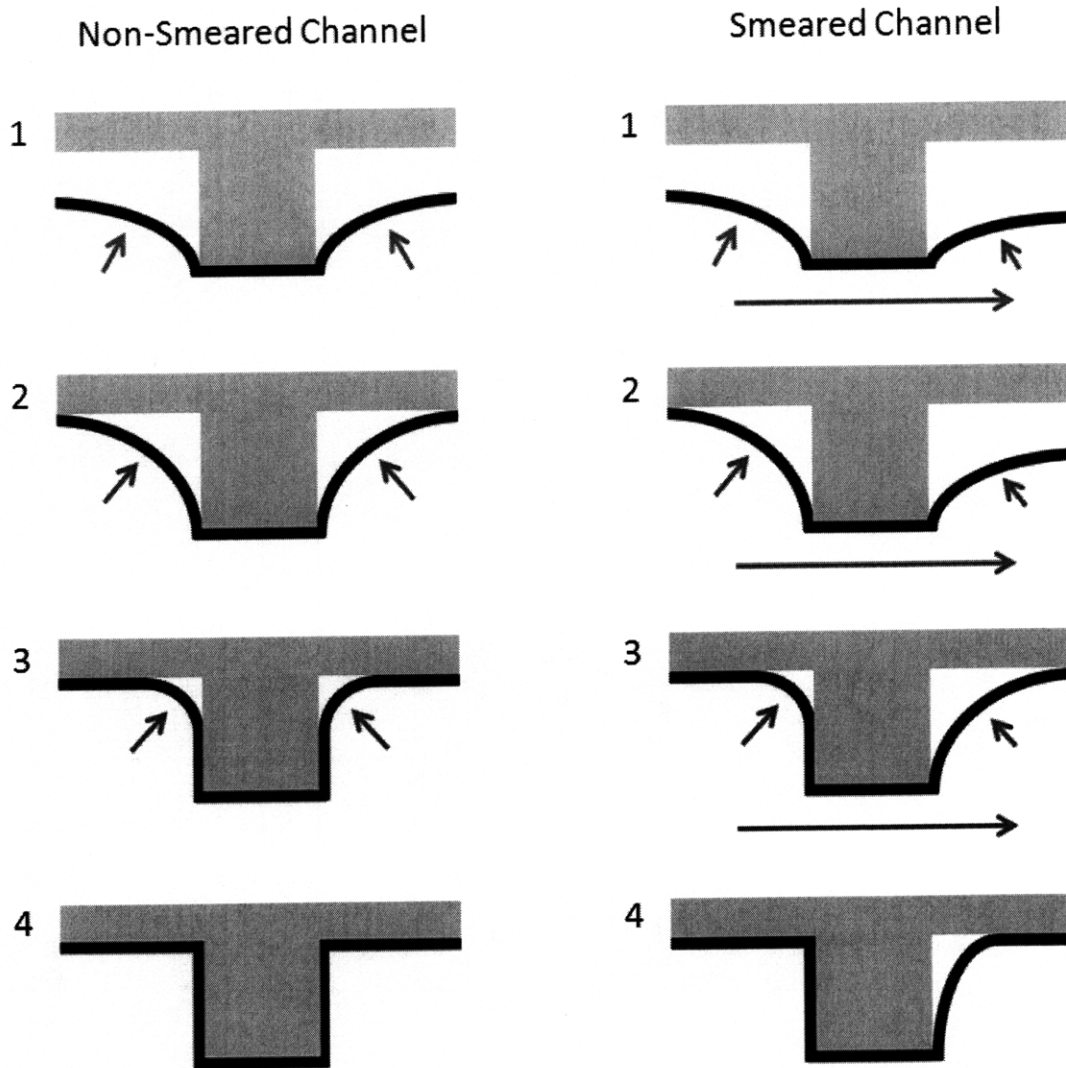


Figure 4-9 Illustration of the effect of bulk material flow on channel formation. The tool is shown in light gray, the part being embossed is black. The dark gray arrows represent material flow.

The images on the left half of figure 4-9 represent the case in which there is no or very little bulk material flow. The two sides of the channel experience similar material flow

into the features, as indicated by the dark gray arrows, resulting in an evenly formed channel. The images on the right half represent the case where there is bulk material flow, indicated by the dark gray arrows below the tool and part. The bulk material flow counteracts the material flow into tool features on the right side of the channel, resulting in less material flow into the features on this side, as indicated on the images by shorter material flow arrows. This creates a channel that is well formed on one side, but unfilled on the other, which corresponds to the appearance of the measured channels.

Bulk material flow also explains several other features of the smearing effect. For figure 4-7(b) the shadow channel is an area of the part that contacted the tool, but was then dragged outward by bulk material flow. The area that had been in contact with the tool partially filled in during the embossing process, but there were residual effects from the contact with the tool, resulting in the shallow shadow channel. As seen in figure 4-10, the sharp channel edge was less affected by bulk material flow because it was more parallel to the flow direction, whereas the curved edge was more perpendicular, and thus material flow counteracted feature filling to a greater degree.

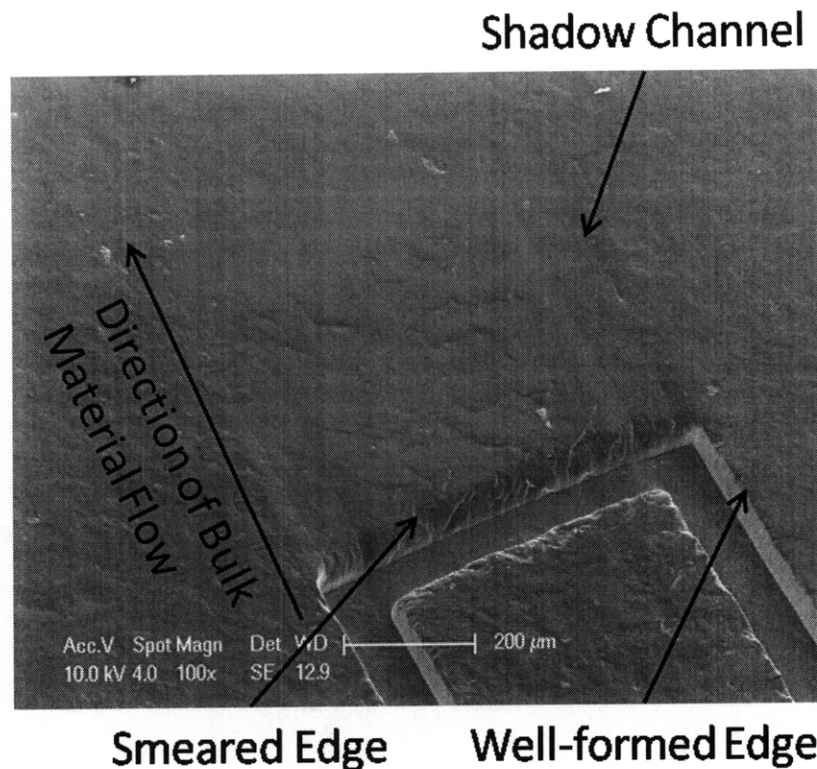
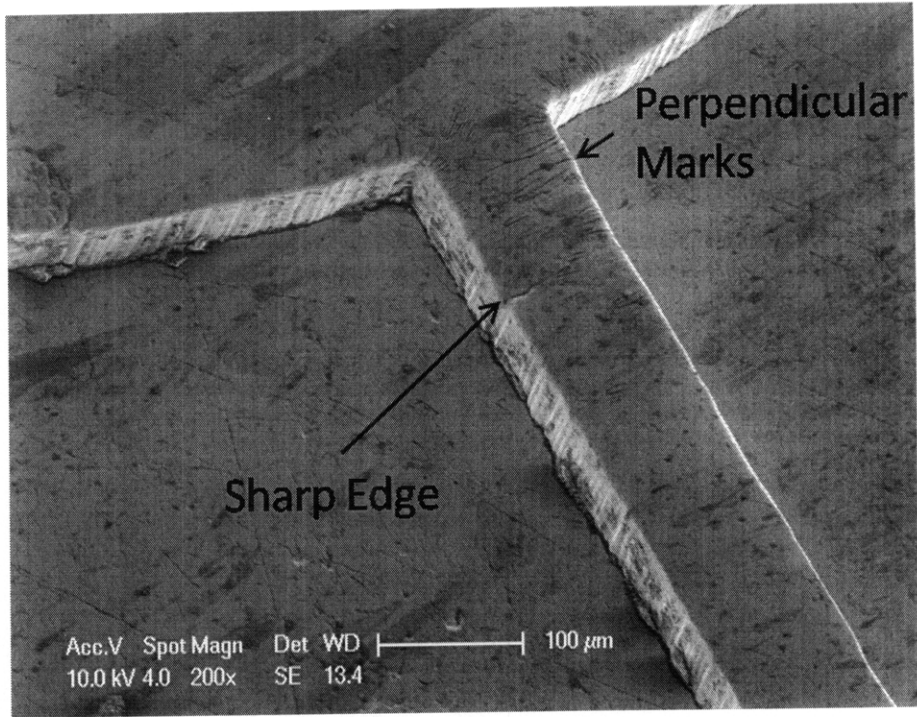


Figure 4-10 SEM image indicating radial flow direction. The smearred edge is perpendicular to flow, while the well formed edge is parallel.

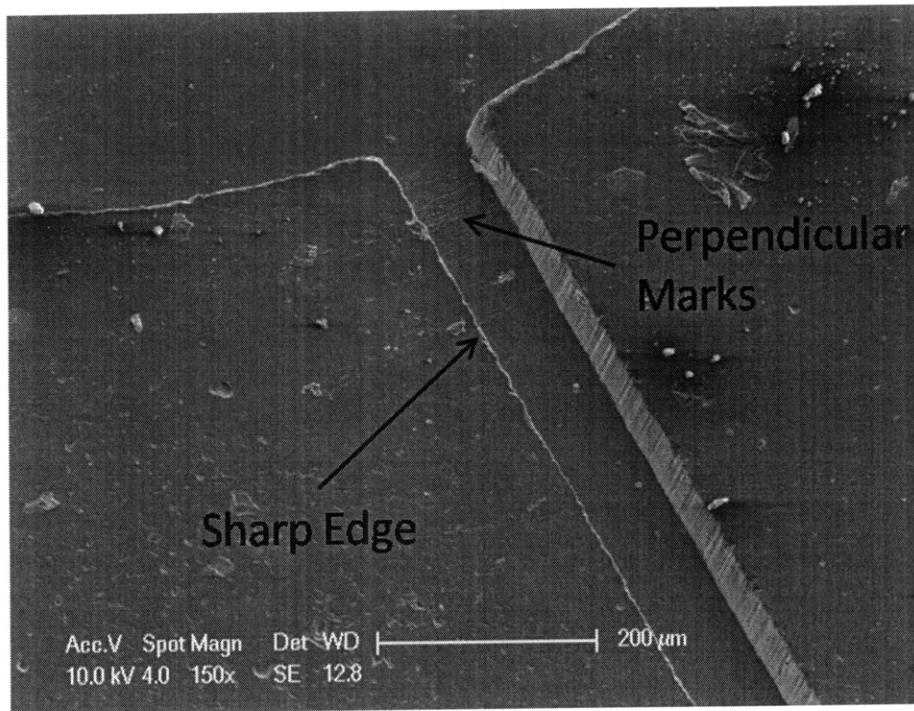
The increased likelihood smearing for channels near the edge of the part is the result of the greater bulk material flow in these locations compared to those near the center of the tool. This effect could be counteracted during the tool design stage by creating tools that don't have features near the tool edges. The temperature dependence of smearing is a product of the fact that at higher temperatures the part material is closer to being molten, meaning that it can flow more readily. This improves the material's ability to flow into tool features, counteracting the effects of bulk material flow.

4.5 Visual Confirmation from SEMs

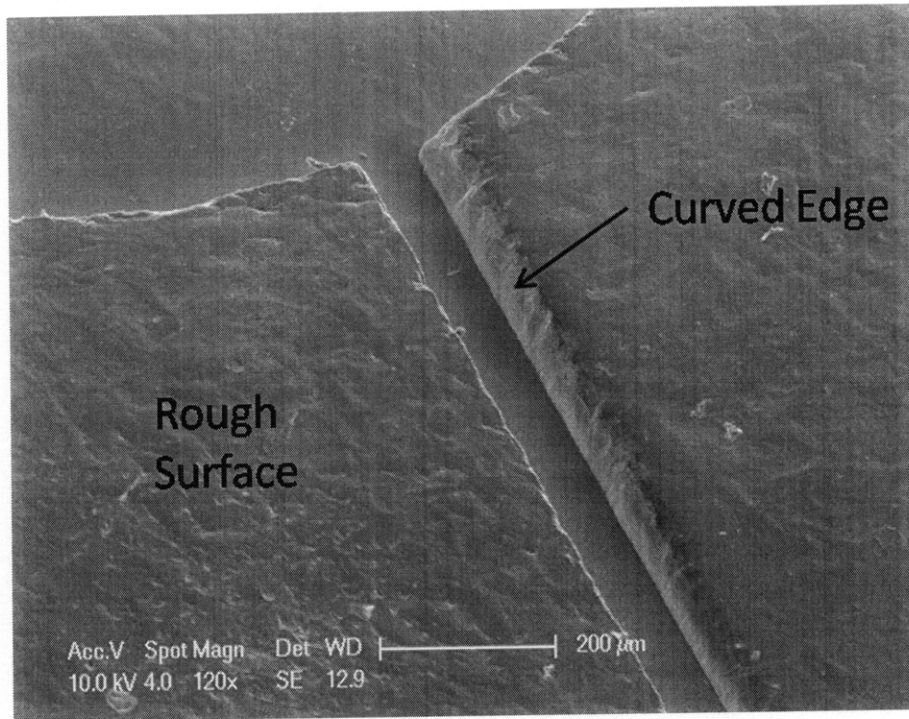
The success of the embossing process can be observed qualitatively from SEM images taken of parts as well as the tool, as seen in figure 4-11.



(a)



(b)



(c)

Figure 4-11 SEM images of the same location on the tool (a), a part embossed at 140° C and 1MPa (b), and a part embossed at 130° C and 2MPa (c).

Figure 4-11 shows the tool used for embossing, figure 4-11(a), as well as the same location on two parts fabricated using the tool, one which is well formed, figure 4-11(b), and one that is not well formed figure 4-11(c). The edges on the well formed part appear clear and sharp, similar to those of the tool, while the walls on the poorly formed part are sloped and the edges are curved in a poor replication of the tool. The surface of the poorly formed part also appears rougher than that of the well formed part, a result of residual texture from the Urethane film. On the better replicated part, this texture was smoothed during the embossing process to match the smooth surface of the tool. The replication for the better formed part was also successful enough to reproduce small features. On the tool, a series of marks perpendicular to the channel are visible near the circular well in the upper portion of the image. These marks were successfully replicated on the well replicated part and are visible on the SEM image.

4.6 Measurement Repeatability

The measurement of parts is composed of two aspects, measurement on the Zygo, and data processing in Gwyddion. The repeatability of the former was investigated by Aaron Mazzeo, a graduate student under Professor Hardt at the Laboratory for Manufacturing and Productivity at MIT. Mazzeo tested the repeatability of measuring PDMS parts formed from an embossed mold by measuring the same location on a single part 20 times and processing the data to extract channel dimensions using a custom script in MatLab [31]. Between measurements, the part was removed from the profilometer stage, and then reloaded, in order to recreate the variability that would take place during the actual measurement process. To this same end, the tilt of the profilometer stage was occasionally adjusted and microscope objectives were switched back and forth. Mazzeo found that the height measurements of the part differed by $0.28\mu\text{m}$, or 0.60% of the measured mean height of $46.49\mu\text{m}$, while the width measurements differed by $0.17\mu\text{m}$, or 0.072% of the average channel width of $237.46\mu\text{m}$ [31]. The repeatability of the Gwyddion measurements was tested in a similar way, by processing a single data file ten times from start to finish. For each run, Gwyddion's embedded rulers were used to select the same profile location on the image, a practice which was also employed when taking measurements. The data was also corrected to remove areas of missing data, shifted so the minimum data point was set to zero, and, in some cases, leveled, just as was described in the Methods section 3.4 above. The step fitting function was used and height and width measurements were determined. For each of the ten runs, the height and width data were identical, indicating that the Gwyddion processing did not increase measurement variation. It is therefore expected that the repeatability of the

measurements in the current study is similar to that found by Mazzeo [31].

5

Conclusions and future work

5.1 Summary

Microfluidic devices have been used for a variety of biological applications, many of which make use the integration of multiple components on a single chip [1-5]. The possibility for large scale integration of such components on microfluidic devices, analogous to that of electrical circuits, is expected to increase the usefulness of such devices even further. Active elements such as valves and pumps have been identified as a crucial component for many microfluidic devices, and for LSI in particular [1, 3]. A common technique for fabricating such active elements is the use of flexible materials to create valves and pumps [2, 6]. Thus far, the most prevalent material used to fabricate flexible active elements has been PDMS. PDMS has many desirable qualities, including high flexibility, easy fabrication techniques, the possibility for rapid prototyping, and biocompatibility. However, the rate at which devices can be fabricated from PDMS is inherently limited by the curing process necessary to create parts, which makes PDMS potentially undesirable for large scale production [7, 8].

Thermoplastic elastomers provide a potential alternative to PDMS for the fabrication of flexible active elements. TPEs are two phase materials that are flexible and rubbery at room temperature, but which can be melted and processed using the same techniques as for traditional thermoplastics, such as injection molding or casting [10-12]. Such processing techniques can achieve greater production rates than casting of PDMS,

making TPEs more viable for large scale production [9]. One potential processing technique to fabricate microfluidic devices from TPEs is hot embossing. The hot embossing process involves heating a material above its glass transition temperature, then imprinting it with a micromachined tool, causing the material to fill the tool features and form a negative replica of the tool [25, 26, 27]. For this investigation, the use of hot embossing to create parts from a particular TPE, Stevens Urethane 1880 was studied.

5.2 Conclusion

This investigation has shown that it is possible fabricate microfluidic devices using hot embossing. In addition, a processing window for the TPE investigated, Stevens Urethane 1880, has been characterized for the specific tool used. The method of characterization employed has been described, and could be utilized in future attempts to characterize the processing windows for hot embossing TPEs. Good results were obtained at temperatures above 140°C and pressures in the range of 1MPa-1.5MPa, although these pressure values would be lower for increased temperatures, with the best replication occurring at 150°C and 1.5MPa. An upper limit on temperature was not found, and the highest temperatures investigated are approaching the point at which the material is molten. This suggests that a fabrication process for which the material is intentionally melted, such as casting, may also be suitable for fabrication of microfluidic devices from TPEs.

5.3 Future work

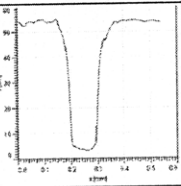
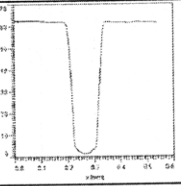
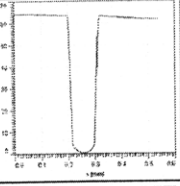
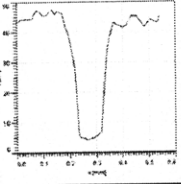
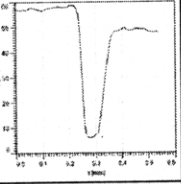
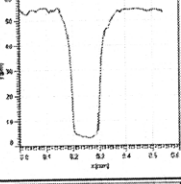
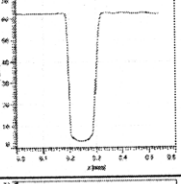
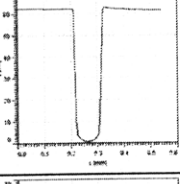
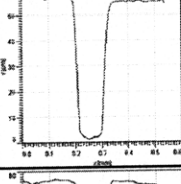
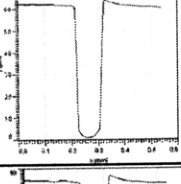
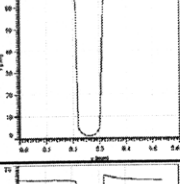
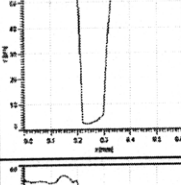
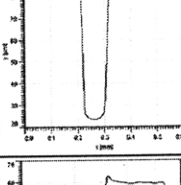
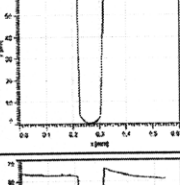
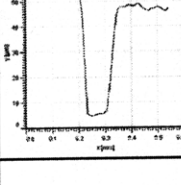
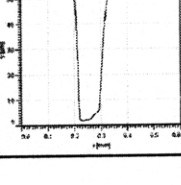
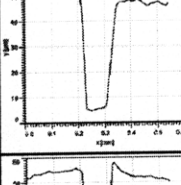
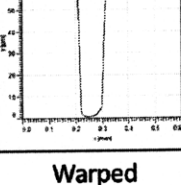
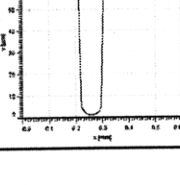
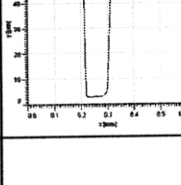
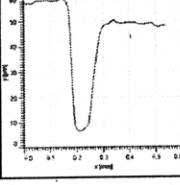
Although determining the processing window for TPEs, specifically Stevens Urethane 1880, is a useful step in the development of hot embossing TPEs for

microfluidic devices, it is by no means the only one. For one thing, this investigation has only examined a single TPE, while a number of other promising materials remain to be characterized. It also addressed only one specific tool, and a study of tools with different feature geometries, such as various widths, depths, or feature densities, remains as a topic for future investigation. Also, de-embossing temperature and hold time were not studied, but may have a significant impact on the quality of parts, especially considering the effects of bulk material flow. In addition, no attempt was made to determine the process variation of hot embossing TPEs. A potential topic for future study would be the variation in channels from part to part for TPEs, and a comparison of this process variation to that for PDMS or traditional thermoplastics. Finally, the fabrication of active elements in TPE microfluidic devices will almost certainly require some sort of bonding, such as a cover plate bonded to the top of the embossed part. While bonding with PDMS has been well studied, bonding TPEs is likely to be more complicated. Stoyanov et.al. have reported successful chemically bonding of an embossed TPE part to a cover plate of the same material [13, 14]. However, this bonding was not thoroughly addressed in their report, and future investigation into this, or other, bonding technology is necessary for the realization of microfluidic TPE active elements.

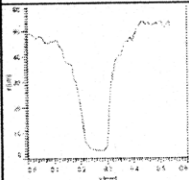
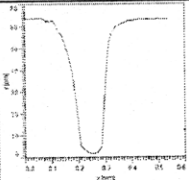
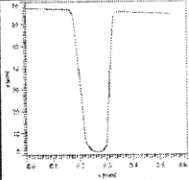
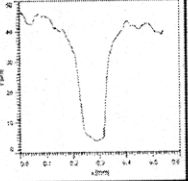
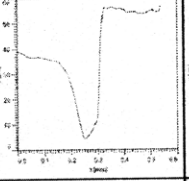
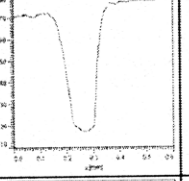
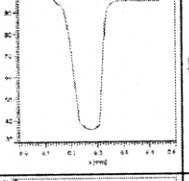
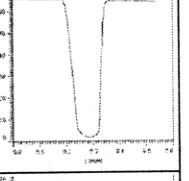
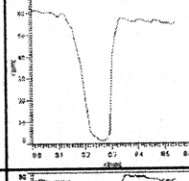
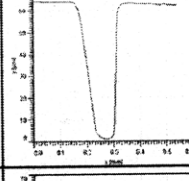
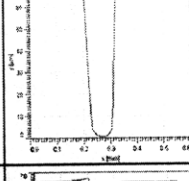
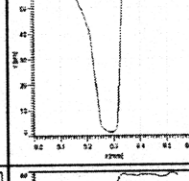
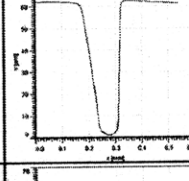
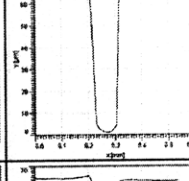
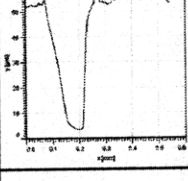
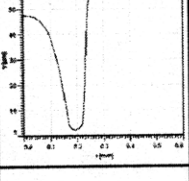
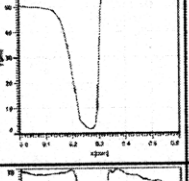
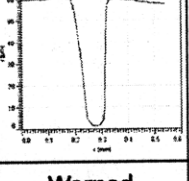
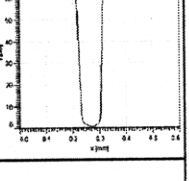
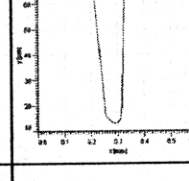
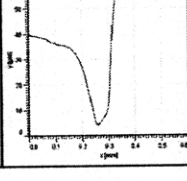
Appendix

A Cross Section Matrices

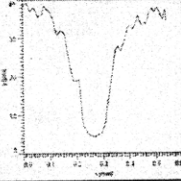
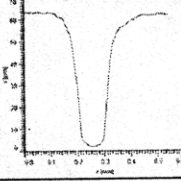
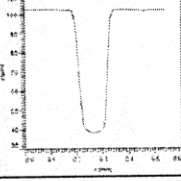
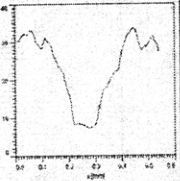
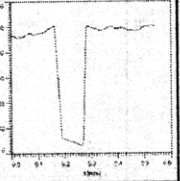
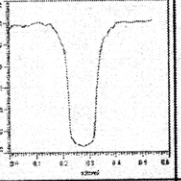
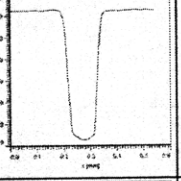
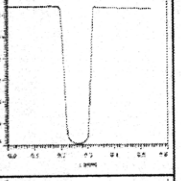
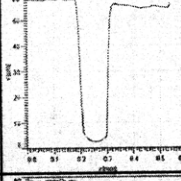
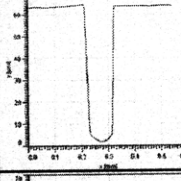
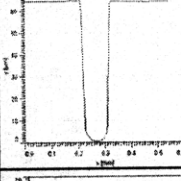
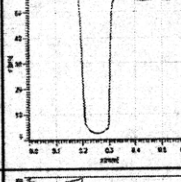
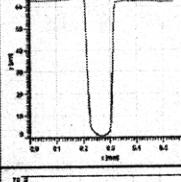
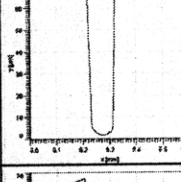
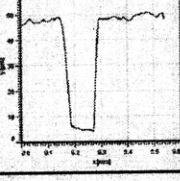
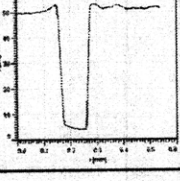
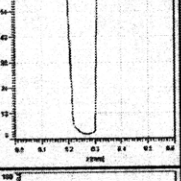
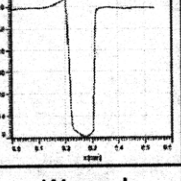
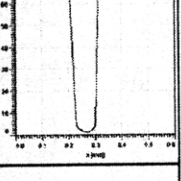
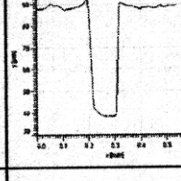
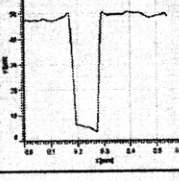
A.1 Matrix for Location 1

Location 1	100°C	120°C	130°C	140°C	150°C
0.25MPa					
0.5MPa					
1.0MPa					
1.5MPa					
2.0MPa					
3.0MPa				Warped	
4.0MPa		Warped			

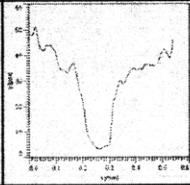
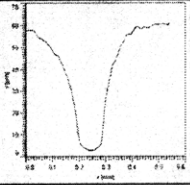
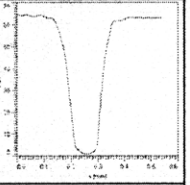
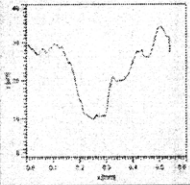
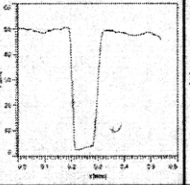
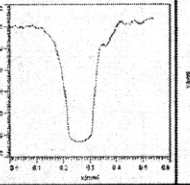
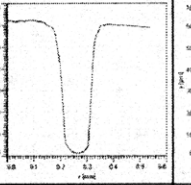
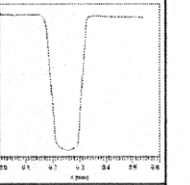
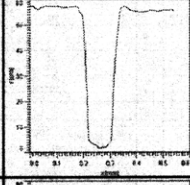
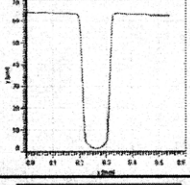
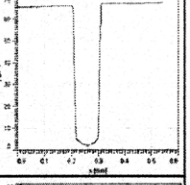
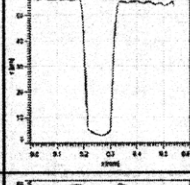
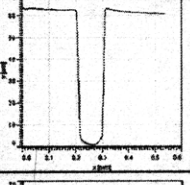
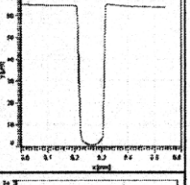
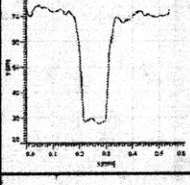
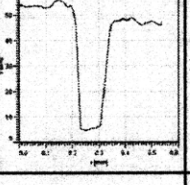
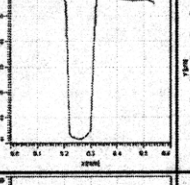
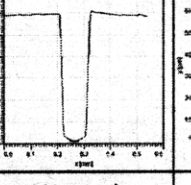
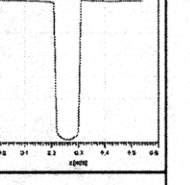
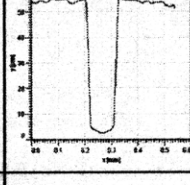
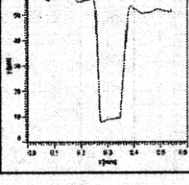
A.2 Matrix for Location 2

Location 2	100°C	120°C	130°C	140°C	150°C
0.25MPa					
0.5MPa					
1.0MPa					
1.5MPa					
2.0MPa					
3.0MPa				Warped	
4.0MPa		Warped			

A.3 Matrix for Location 3

Location 3	100°C	120°C	130°C	140°C	150°C
0.25MPa					
0.5MPa					
1.0MPa					
1.5MPa					
2.0MPa					
3.0MPa				Warped	
4.0MPa		Warped			

A.4 Matrix for Location 4

Location 4	100°C	120°C	130°C	140°C	150°C
0.25MPa					
0.5MPa					
1.0MPa					
1.5MPa					
2.0MPa					
3.0MPa				Warped	
4.0MPa		Warped			

B Success of Part Formation

B.1 Average Width and Depth of Parts

Average Depth:

	0.25MPa	0.5MPa	1MPa	1.5MPa	2MPa	3MPa	4MPa
100°C		27.55μm			44.43μm		45.47μm
120°C		43.46μm			46.91μm		Warped
130°C	36.75μm	54.07μm	54.22μm	52.73μm	53.65μm	51.82μm	
140°C	55.13μm	59.03μm	61.01μm	60.69μm	58.29μm	Warped	
150°C	62.82μm	62.27μm	64.02μm	63.76μm	63.02μm		

Average Width:

	0.25MPa	0.5MPa	1MPa	1.5MPa	2MPa	3MPa	4MPa
100°C		112.87μm			101.61μm		86.70μm
120°C		87.53μm			97.67μm		Warped
130°C	109.21μm	111.18μm	107.52μm	107.52μm	91.78μm	95.13μm	
140°C	108.93μm	108.36μm	94.79μm	87.53μm	89.51μm	Warped	
150°C	106.40μm	102.45μm	86.41μm	84.125μm	79.87μm		

B.2 Average Width and Depth of Tool

Location	height (μm)	avg height (μm)	width (μm)	avg width (μm)
3	66.47	66.41	78.81	80.69
2	66.76	0.39	82.18	1.72
4	65.992		81.07	

B.3 Location Specific Information

Values are in μm unless otherwise indicated. The “Diff. tool” category is the difference between the depth measurement for the part and that for the tool. The “Uniform” column is the difference between the largest and smallest values measured for height or width.

10-Jun	Temp (C)	Press. (MPa)	Smear	Depth	Diff. tool	Uniform	Width	Diff. tool	Uniform
1_01	100	0.5	n	39.832	-26.578	24.038	109.21	28.52	28.14
1_02			n	35.868	-30.542		101.33	20.64	
1_03			n	18.699	-47.711		111.46	30.77	
1_04			n	15.794	-50.616		129.47	48.78	
2_01	120	0.5	y	46.654	-19.756	9.479	77.68	-3.01	19.14
2_02			y	37.175	-29.235		79.93	-0.76	
2_03			n	43.817	-22.593		96.82	16.13	
2_04			n	46.198	-20.212		95.69	15	
3_01	120	2	meh	51.225	-15.185	6.832	95.7	15.01	33.77
3_02			y	45.195	-21.215		77.69	-3	
3_03			n	46.823	-19.587		105.83	25.14	
3_04			n	44.393	-22.017		111.46	30.77	
4_01	100	2	y	46.211	-20.199	5.303	101.33	20.64	22.52
4_02			y	46.811	-19.599		86.69	6	
4_03			n	43.191	-23.219		109.2	28.51	
4_04			n	41.508	-24.902		109.21	28.52	
5_01	100	4	y	56.254	-10.156	18.592	75.44	-5.25	24.77
5_02			y	37.662	-28.748		74.31	-6.38	
5_03			n	43.195	-23.215		97.95	17.26	
5_04			meh	44.778	-21.632		99.08	18.39	
8-Jul	Temp (C)	Press. (MPa)	Smear	Depth	Diff. tool	Uniform	Width	Diff. tool	Uniform
1_01	120	4							
1_02									
1_03									
1_04									
2_01	130	0.5	meh	55.157	-11.253	5.033	112.58	31.89	6.75
2_02			y	55.393	-11.017		106.96	26.27	
2_03			n	55.373	-11.037		111.46	30.77	
2_04			meh	50.36	-16.05		113.71	33.02	
3_01	140	0.5	n	59.128	-7.282	0.86	105.83	25.14	4.51
3_02			y	58.569	-7.841		106.95	26.26	
3_03			n	59.429	-6.981		110.33	29.64	
3_04			n/meh	58.999	-7.411		110.34	29.65	

4_01	130	2	y	55.23	-11.18	7.079	87.82	7.13	11.25
4_02			y	48.69	-17.723		87.91	7.22	
4_03			n	54.9	-11.51		92.32	11.63	
4_04			n	55.77	-10.644		99.07	18.38	
4_05	130	1	n/meh	54.69	-11.725	0.983	108.09	27.4	10.12
4_06			y	53.7	-12.708		101.33	20.64	
4_07			n	54.36	-12.05		111.45	30.76	
4_08			n	54.15	-12.257		109.21	28.52	
4_09	140	1	n	60.74	-5.668	0.544	87.82	7.13	16.88
4_10			y	60.84	-5.572		94.57	13.88	
4_11			n	61.29	-5.124		92.07	11.38	
4_12			n	61.2	-5.215		104.7	24.01	
4_13	130	1.5	meh	53.27	-13.136	0.917	103.58	22.89	13.51
7_02			y	52.57	-13.842		90.07	9.38	
7_03			n	52.71	-13.697		97.95	17.26	
7_04			n	52.36	-14.053		103.33	22.64	
8_01	140	1.5	n	60.96	-5.447	3.288	85.56	4.87	5.63
8_02			y	58.63	-7.781		86.69	6	
8_03			n	61.92	-4.493		91.19	10.5	
8_04			n	61.27	-5.145		86.69	6	
9_01	130	0.25	n	50.23	-16.177	24.821	114.84	34.15	10.14
9_02			y	40.91	-25.502		110.33	29.64	
9_03			n	25.41	-40.998		104.7	24.01	
9_04			n	30.45	-35.959		106.95	26.26	
10_01	140	0.25	n	60.15	-6.26	14.213	109.2	28.51	3.37
10_02			y	57.51	-8.897		106.96	26.27	
10_03			n	56.92	-9.493		110.33	29.64	
10_04			meh	45.94	-20.473		109.21	28.52	
11_01	150	0.25	n	62.57	-3.844	3.304	95.7	15.01	16.89
11_02			y	64.1	-2.309		109.21	28.52	
11_03			n/meh	63.8	-2.607		108.08	27.39	
11_04			n	60.8	-5.613		112.59	31.9	
8-Aug	Temp (C)	Press. (MPa)	Smear	Depth	Diff. tool	Uniform	Width	Diff. tool	Uniform
1_01	130	3	n	51.19	-15.216	5.374	99.07	18.38	23.64
1_02			y	54.92	-11.495		78.81	-1.88	
1_03			n	49.54	-16.869		100.2	19.51	
1_04			n	51.64	-14.773		102.45	21.76	
2_01	140	2	n/meh	58.01	-8.398	1.15	87.82	7.13	10.14
2_02			y	57.75	-8.665		83.31	2.62	
2_03			n	58.9	-7.515		93.45	12.76	
2_04			n	58.5	-7.908		93.45	12.76	

3_01	150	0.5	n	61.49	-4.916	1.498	88.94	8.25	23.64
3_02			y	62.99	-3.418		109.2	28.51	
3_03			n	62.87	-3.537		99.08	18.39	
3_04			y	61.72	-4.69		112.58	31.89	
4_01	150	1	n	63.71	-2.702	1.083	82.19	1.5	11.26
4_02			y	64.7	-1.714		93.45	12.76	
4_03			n	63.61	-2.797		87.81	7.12	
4_04			n	64.08	-2.334		82.19	1.5	
5_01	140	3							
5_02									
5_03									
5_04									
6_01	150	2	n	62.32	-4.091	1.268	70.68	-10.01	14.89
6_02			n	63.15	-3.264		83.31	2.62	
6_03			n	63.02	-3.393		85.57	4.88	
6_04			n	63.59	-2.823		79.93	-0.76	
7_01	150	1.5	n/meh	63.26	-3.15	0.966	79.94	-0.75	7.87
7_02			n/meh	64.23	-2.184		87.81	7.12	
7_03			n/meh	63.88	-2.53		84.44	3.75	
7_04			n	63.71	-2.701		84.31	3.62	

B.4 Success in Each Criteria

Temp	Pressure	Number	Bad/ Good	Height	Width	Uniform
100	0.5	6-10_1	bad	unfilled	too wide	no
100	2	6-10_4	bad	unfilled	too wide	no
100	4	6-10_5	bad	unfilled	10% 2, 20% all	no
120	0.5	6-10_2	bad	unfilled	10% 2, 20% all	no
120	2	6-10_3	bad	unfilled	too wide	no
120	4	7-8_1	bad	warped	warped	warped
130	0.25	7-8_9	bad	unfilled	too wide	height no, width yes
130	0.5	7-8_2	bad	unfilled	too wide	height no, width yes
130	1	7-8_5	bad	unfilled	too wide	yes
130	1.5	7-8_7	bad	unfilled	too wide	yes
130	2	7-8_4	bad	unfilled	10% 3, 20% all	height no, width yes
130	3	8-8_1	bad	unfilled	too wide	no
140	0.25	7-8_10	bad	15% save one	too wide	height no, width yes
140	0.5	7-8_3	bad	15%	too wide	yes
140	1	7-8_6	borderline	10%	15% 2, 20% 3	height yes, width no
140	1.5	7-8_8	good	10% save one	10% 3, 20% all	yes
140	2	8-8_2	borderline	15%	15% 2, 20% all	yes
140	3	8-8_5	bad	warped	warped	warped
150	0.25	7-8_11	bad	5% save one	too wide	height yes, width no
150	0.5	8-8_3	bad	10%	too wide	height yes, width no
150	1	8-8_4	good	5%	10% 3, 20% all	yes
150	1.5	8-8_7	good	5%	0.1	yes
150	2	8-8_6	borderline	5% 2, 10% all	10% 3, 15% all	yes

References

- 1 J.W. Hong and S.S. Quake, "Integrated Nanoliter Systems." *Nature Biotechnology*, v 21, n 10, October 2003, p 1179-1183.
- 2 D.R. Reyes, D. Lossifidis, P.A. Auroux, A. Manz, "Micro Total Analysis Systems. 1. Introduction, Theory, and Technology." *Analytical Chemistry*, v 74, n 12, June 2002, p 2623-2636.
- 3 T. Thorsen, S.J. Maerkl, S.R. Quake, "Microfluidic Large-Scale Integration." *Science*, v 298, October 2002, p 580-584.
- 4 L. Chen, A. Manz, P.J.R Day, "Total nucleic acid analysis integrated on microfluidic devices." *Lab on a Chip*, v 7, July 2007, p 1413-1423.
- 5 P. Mitchell, "Microfluidics – downsizing large-scale biology." *Nature Biotechnology*, v 19, August 2001, p 717-721.
- 6 S. Haeberle and R. Zengerle, "Microfluidic platforms for lab-on-a-chip applications." *Lab on a Chip*, v 7, n 9, September 2007, p 1081-1220.
- 7 J.C. McDonald and G.M. Whitesides, "Poly(dimethylsiloxane) as a Material for Fabricating Microfluidic Devices." *Accounts of Chemical Research*, v 35, n 7, July 2002 p 491-499.
- 8 M.A. Unger, H. Chou, T. Thorsen, A. Scherer, S.R. Quake, "Monolithic Microfabricated Valves and Pumps by Multilayer Soft Lithography." *Science*, v 288, n 113, April 2000, p 113-116.
- 9 A.D. Mazzeo, M. Dirckx, D.E. Hardt, "Process Selection for Microfluidic Device Manufacturing." Unpublished
- 10 M. Morton, *Rubber Technology*, Third Ed. Kluwer Academic Publishers, 1995.
- 11 T. Whelan, *Polymer Technology Dictionary*, Springer, 1993.
- 12 J.G. Drobny, *Handbook of Thermoplastic Elastomers*, William Andrew Publishing/Plastics Design Laboratory, 2007.
- 13 I. Stoyanov, M. Tewes, M.Koch, M. Löhndorf, "Microfluidic devices with integrated active valves based on thermoplastic elastomers." *Microelectrical Engineering*, v 83, 2006, p 1681-1683.
- 14 I. Stoyanov, M. Tewes, M.Koch, M. Löhndorf, "Low-cost and chemical resistant microfluidic devices based on thermoplastic elastomers for a novel biosensor system" *Materials Research Society Symposium Proceedings*, v 872, 2005, J11.4.1-J11.4.6.

- 15 Dow Sylgard Data Sheets: <http://www.dow.com/>
- 16 K. Choi, J.A. Rogers, "A Photocurable Poly(dimethylsiloxane) Chemistry Designed for Soft Lithographic Molding and Printing in the Nanometer Regime," *Journal of the American Chemical Society*, v 125, 2003, p 4060-4061.
- 17 Stevens Urethane Data Sheet: Provided by company
- 18 Lubrizol Estane Data Sheets: <http://www.estane.com/tradename/estane-58000-series.asp>
- 19 Lubrizol website: <http://www.estane.com/process/film-and-sheet.asp>
- 20 Lubrizol Tecoflex Data Sheets: <http://www.estane.com/tradename/tecoflex-clear-grade.asp>
- 21 Dow Pellethane Data Sheets:
<http://plastics.dow.com/plastics/ap/prod/specialty/pellethane.htm>
- 22 SK Chemicals Skythane Data Sheets:
<http://www.skchemicals.com/english2/product/special/ind/thane/Product010102.asp>
- 23 DSM Armitel Data Sheets: http://www.dsm.com/en_US/html/dep/armitel.htm
- 24 Arkema Pebax Data Sheets: <http://www.pebax.com/>
- 25 Q. Wang, D.E. Hardt, "Processing Window Identification and Process Variability Study of Micro Embossing," *ICOOM*, n 57, 2006.
- 26 M. Dirckx, *Design of a Fast Cycle Time Hot Micro-Embossing Machine*, S.M. Thesis, Massachusetts Institute of Technology, 2005.
- 27 M. Hecke and W.K. Schomburg, "Review on micromolding of thermoplastic polymers." *Journal of Micromechanics and Microengineering*, v 14, 2004, p R1-R14.
- 28 Roos, T. Luxbacher, T. Glinsner, K. Pfeiffer, H. Schulz, and H. C. Scheer, "Nanoimprint lithography with a commercial 4 inch bond system for hot embossing," presented at SPIE's 26th Annual International Symposium Microlithography, Feb. 25 – March 2, 2001.
- 29 D. Henann and L. Anand, *Acta Materialia* 56 (2008) 3290-3305.
- 30 Gwyddion Documentation: <http://gwyddion.net/documentation/user-guide/index.html>

31 A.D. Mazzeo and D.E. Hardt, "Toward the Manufacture of Micro and Nano Features with Curable Liquid Resins: Mold Materials and Part-to-part Dimensional Variation" Unpublished.